August 5, 1998

Unpublished Manuscript

Inorganic Carbon Variations in Surface Ocean Water near Bermuda

Timothy J. Lueker, Charles D. Keeling, Peter R. Guenther,
and Martin Wahlen

Scripps Institution of Oceanography
University of California, San Diego
La Jolla, CA 92093

Willem G. Mook

Netherlands Institute for Sea Reseach (NIOZ)
Texel, The Netherlands 89505

Abstract

Time series of dissolved inorganic carbon (DIC) and of titration alkalinity (TA) in the surface ocean at Hydrostation 'S' near Bermuda have been obtained from water samples collected from September 1983 through March, 1997 and returned to our laboratory for analysis. The concentration of DIC was determined by vacuum extraction of acidified seawater followed by manometric assay of the evolved CO_2. TA was determined by potentiometric titration. The seawater temperature at the time of sampling, and the measured salinity, DIC and TA were used to calculate the partial pressure of CO_2 (pCO_2) of the seawater. The reduced ^{13}C / ^{12}C ratio, $\delta^{13}C$ of the CO_2 gas extracted from the samples was determined with stable isotope mass spectrometers. The DIC, pCO_2, and $\delta^{13}C$ data exhibit pronounced seasonal cycles, interannual variations, and secular trends. These data were fitted to harmonic functions to represent the seasonal cycles, and linear functions to represent the secular trends. The results indicate annual changes of 0.76 μmol kg^{-1} in DIC, -0.026 ‰ in $\delta^{13}C$, and 1.48 μatm in pCO_2. The secular trends were also evaluated from data corresponding to the observed annual minima in surface ocean temperature. At these times annual changes on average were 0.93 μmol kg^{-1} in DIC, -0.023 ‰ in $\delta^{13}C$, and 1.55 μatm yr^{-1} in pCO_2. DIC and pCO_2 increased at rates similar to those predicted

from ocean carbon cycle model simulations; $\delta^{13}C$, however, changed more rapidly than predicted. Pronounced interannual variability was observed in DIC, $\delta^{13}C$, and pCO_2 data, most of which was correlated with annual minima in surface ocean temperature.

Introduction

Time-series measurements of the variations of carbon composition in the atmosphere, oceans, and terrestrial biosphere are essential for elucidating linkages between climate and the global carbon cycle (e.g. Keeling et al., 1989; Tans et al., 1990; Tans et al., 1993; Keeling et al., 1993). Improved understanding of the ocean carbon cycle is particularly important in order to increase the confidence in estimations of the net CO_2 flux into the oceans of fossil fuel CO_2, and to understand the potential for future changes in the natural cycles and forcing of the air-sea exchange of CO_2 (Sigenthaler and Sarmiento, 1993; Sarmiento and Lequere, 1996). The value of time series measurements of ocean carbon chemistry has been demonstrated in studies of the perturbation of the ocean carbon cycle resulting from increasing atmospheric CO_2 (Keeling, 1993; Lueker and Keeling, 1994; Gruber et al., 1996; Bates et al., 1996; Winn et al., 1996; Bacastow et al., 1996; Winn et al., 1998). As these time series continue, the uncertainties due to sampling frequency and synoptic scale variability can be more reliably ascertained, and hence their value for validating ocean carbon cycle models increases.

Here, we report time series measurements of inorganic carbon in the surface ocean, begun in 1983 with samples collected from the Sargasso Sea near the Island of Bermuda. Seawater sampled at Hydrostation "S" (32° 10'N, 64°30'W) has been analyzed for dissolved inorganic carbon (DIC), titration alkalinity (TA), and the $\delta^{13}C$ of the DIC. Earlier portions of this time series have already been reported in investigations of the carbon cycle in the Sargasso Sea (Keeling, 1993; Lueker and Keeling, 1994; Bacastow et al., 1996; Marchal et al., 1996; Gruber and Keeling, 1998; Gruber et al., 1998). In this report we first discuss instrumentation and analytical procedures and then present data for DIC, TA, $\delta^{13}C$, temperature and salinity, measured from samples collected through March 1997. We use the DIC and TA data to calculate

the CO_2 partial pressure at the ocean's surface (pCO_2) utilizing formulations of the carbonic acid dissociation constants K_1 and K_2.

Subsequent to our measurements, in the late 1980's, the Joint Global Ocean Flux Study (JGOFS) established time series studies at two additional stations, "BATS", approximately 85 km SE of Hydrostation 'S', and "ALOHA", in the north Pacific subtropical gyre, near Hawaii, where intensive investigations of the ocean carbon cycle continue (Michaels and Knap, 1996; Karl and Lucas, 1996; Bates et al., 1996; Winn et al., 1996; Winn et al., 1998; Bates et al., 1998; refs). We have also measured DIC, TA, and $\delta^{13}C$ at these locations. We will discuss our results from Hydrostation 'S' in the context of previously reported observations from BATS, and discuss differences observed in the DIC data from the two time series.

Time Series Location and Sampling Procedures

Michaels and Knapp (1996) have recently summarized the oceanographic characteristics of Hydrostation 'S' and the BATS site in detail. Hydrostation 'S' is characterized by surface currents usually flowing toward the southwest at less than 5 cm sec^{-1}, however the area is often influenced by mesoscale eddies emanating from the gulf stream (Worthington, 1975; Lai and Richardson, 1977 Siegel et al., 1994; Olbers et al., 1995). The hydrography recorded in repeated profiles of temperature, salinity, and dissolved oxygen demonstrates a seasonal cycle in ocean surface temperature of nearly 10 $^\circ$C, and decadal scale variability in the depth of winter convective mixing and surface water ventilation (refs; Talley and Raymer, 1982; Michaels and Knap, 1996; Joyce et al., 1998). Typically, the depth of the mixed-layer varies seasonally from less than 10 m to greater than 200 m while the euphotic layer varies between 90 and 140 meters (Talley and Raymer, 1982; Michaels et al., 1994; Michaels and Knap, 1996; Joyce et al., 1998). Numerous studies including estimates of net community production and oceanic carbon cycling have been based on observations recorded at Hydrostation 'S' and at the BATS site (e.g. Menzel and Ryther, 1960; Jenkins 1982, Jenkins and Goldman, 1985; Platt and Harrison, 1985; Deuser, 1986; Spitzer and Jenkins, 1989; Bisset et al., 1994; Deuser et al., 1995; Marchal et al., 1996;

Doney et al., 1996; Bacastow et al., 1996; Bisset et al., 1997; Gruber and Keeling, 1998; Gruber et al., 1998).

To obtain seawater samples for this study, we have relied on personnel from the Bermuda Biological Station for Research to collect seawater samples for us. Approximately once a month two pairs of one-liter reagent bottles were filled with seawater drawn from 10 liter Niskin bottles tripped at approximately 2 and 10 meter depths. Each sample was promptly poisoned with 100 μl of saturated $HgCl_2$ solution and then sealed with a greased stopper. Upon arrival at our laboratory, the bottles were inspected for evidence of gas leakage, then stored in the dark at 5 $^\circ$C prior to analysis. Samples were usually analyzed within 6 months of the sample date.

Analytical Procedures

The DIC of the seawater samples is determined in our laboratory using a vacuum extraction/manometric procedure derived from the work of Wong (1970; Keeling et al, 1998). A weighed aliquot of seawater from each sample bottle is acidified under vacuum and the resulting CO_2 gas is extracted in a condensation trap cooled with liquid nitrogen. The CO_2 gas is purified by repeated sublimations and then introduced into a mercury manometer. In the manometer the CO_2 gas pressure, temperature, and volume are measured. The amount of CO_2 is determined from the measured properties using an equation of state.

After the aliquots of DIC have been taken from the sample bottles, the TA of the seawater samples is determined using a potentiometric procedure based on the work of Edmond (1970), the GEOSECS titration systems (Bradshaw et al., 1981) and the recommendations of Dickson (1981). The titration data are processed using a non-linear least squares fit of the emf and titrant volume data to a proton condition model (Dickson, 1981; DOE, 1994).

After manometric assay of the extracted DIC, the $\delta^{13}C$ of the CO_2 gas is determined. The CO_2 gas extracted from samples collected prior to September 1990 was shipped to the Centrum voor Isotopen Onderzoek at the University of Groningen, where $\delta^{13}C$ was determined, as

described by Mook and Grootes (1973) and Mook et al. (1983). Samples collected after September, 1990 were analyzed at the Scripps Institution of Oceanography using a VG Prism isotope ratio mass spectrometer. A detailed description of the instrumentation and procedures used for analysis of the DIC, TA and the $\delta^{13}C$ of the DIC at Scripps, as well as a description of the standardization procedures used for measurements is given in Appendix A.

After analyses of DIC and TA is completed, the one liter pyrex bottles, typically still containing at least 500 ml of seawater, are sampled for salinity and inorganic nutrient analyses. The analyses are performed by the Oceanographic Data Facility at the Scripps Institution of Oceanography using standard analytical methodologies (Gordon et al., 1993). The salinity data measured in our sample bottles were compared with salinity data published by the Bermuda Biological Station for Research (data available at WWW.BBSR.EDU). Of 280 salinity analyses, the mean difference was 0.0008 with a s.d. of 0.015 (8 differences over 0.1 were rejected). The results of nutrient measurements on seawater sub-sampled from our Hydrostation 'S' samples are available upon request.

Description of the Data

Our DIC, TA, and $\delta^{13}C$ measurements of seawater from Hydrostation 'S' are presented in Table 1[*] as the averages and differences of the pairs of duplicate samples. The letter "S", appearing in the table indicates single sample analyses.

---

[*] For 106 analyses of TA made prior to May, 1986, we report only 39. The unreported data are rejected because of evidence of alkalinity contamination from the type of bottles in which these samples were inadvertently stored.

By analyzing duplicate samples collected from the same niskin we were able to estimate the standard deviations of the analyses with the formula (Laitinen, 1960)

(8) $\sigma_m = \frac{1}{2} \left\{ \left[\Sigma_i(\Delta_i^2) \right] / n \right\}^{1/2}$

where Δ denotes the difference between duplicate measurements of the Niskin sample, (i) and n denotes the number of duplicates. Based on duplicate sample differences, we found σ_m to be 0.56 μmol kg^{-1} for DIC, 1.03 μmol kg^{-1} for TA, and 0.014 ‰ for δ^{13}C. The reported DIC data have an inaccuracy estimated to be 1.0 μmol kg^{-1}, based on manometric standardizations, and an independent evaluation by Dickson, based on inter-laboratory comparisons of coulometric analyses of Certified Reference Materials (Keeling et al., 1986; Dickson, 1992, Keeling et al., 1998). We estimate the inaccuracy of the alkalinity measurements, calibrated against titrations of sodium carbonate solutions (see Appendix A), and checked against the TA analysis method of Dickson, to be 2 μmol kg^{-1} (Lueker, 1998; Dickson et al., 1998). We estimated the inaccuracy of the δ^{13}C values with respect to carbonate standard, "PDB" (Craig, 1957) to be 0.1‰ based principally on the standards, NBS-16, NBS-17, and NBS-19, using procedures described in Appendix A and by Bollenbacher et al. (1998).

Salinity variations at Station 'S', shown in the top panel of Figure A, are mainly attributable to local evaporation and precipitation, or to inhomogenieties in the surface ocean sampled at Hydrostation 'S', such as variability resulting from eddies generated by the gulf stream (e.g. Bates et al., 1996; Michaels and Knapp; 1996). The short-term salinity changes are superimposed on a decade long trend of increasing salinity. We removed the variations in DIC and TA attributable to a first order to the effects of the variability in salinity by normalizing these data to a constant salinity of 36.6[†], as shown in Figure A (Keeling , 1993; Bates et al., 1996). The normalized DIC data, denoted sDIC, exhibit a regular seasonal cycle, with the highest values occurring in late winter or early spring, and the lowest values occurring in late summer or early

autumn. In contrast, the normalized TA data, denoted sTA, are seasonally invariant, but reveal

episodic reductions, possibly resulting from planktonic calcification superimposed on the

relatively constant background values (Keeling, 1993; Bates et al., 1996). Similar patterns in

sDIC and sTA have been observed at the BATS time series station (Bates et al., 1996).

The seasonal cycle in sDIC is nearly opposite in phase to the seasonal cycle in ocean

temperature, as shown in the top two panels of Figure B. The maxima and minima in the seasonal

cycle of sDIC vary interannually both in magnitude and in seasonal timing. The full extent of

variability in sDIC is difficult to establish because the sampling interval is longer than the time-

scale of short-term variability which affects the physical and biological processes determining

DIC levels (Michaels et al., 1994a; Michaels et al. 1995; Siegel et al., 1995, Bates et al., 1996;

Bates et al., 1998).

Isotopic measurements of $\delta^{13}C$ of DIC are displayed in the third panel of Figure B (from the

top), with the scale inverted to facilitate comparison with variations in the sDIC and pCO_2 data.

There is a distinct seasonal cycle with an amplitude of about 0.20 ‰ and also a pronounced

secular trend towards more negative values.

The partial pressure of CO_2 of the water samples pCO_2, was calculated from DIC, TA[‡],

temperature, and salinity, using an iterative calculation described by Bacastow (1981). The values

of the carbonic acid dissociation constants K_1 and K_2 used in the calculation were based on the

measurements of Mehrbach et al. (1973), reformulated on the pH_T scale by Dickson (pers. com.,

1998; formulas provided in Appendix A). These formulations of K_1 and K_2 were checked against

laboratory seawater equilibration studies that determined the ratio K_1/K_2 from measurements of

$f(CO_2)$, DIC and TA (Lueker, 1998). The uncertainty in calculated pCO_2 attributable to

---

[†] Salinity data are expressed as dimensionless quantities approximately equivalent to parts per thousand by weight, after UNESCO, 1985.

[‡] When alkalinity data were unavailable, mainly before May, 1986, a value of sTA representative of the mean sTA values of 2285.40 $\mu mol\ kg^{-1}$ was used to calculate pCO_2. The uncertainty in the calculation of individual values of pCO_2, by the substitution of average TA for specific data, is estimated to be 3.3 μatm, based on the observed scatter in observed sTA data.

inaccuracy in K_1 and K_2 was determined to be ± 6 µatm (1 s.d.) (Lueker, 1998). Additional equations necessary for calculating the contributions to TA of borate, silicate, phosphate, and hydroxide ion are also listed in Appendix A (DOE, 1994).

To illustrate the direction and potential magnitude of air-sea exchange of CO_2, the ocean pCO_2 data are compared with atmospheric CO_2 data in Figure C. For this illustration, monthly average atmospheric CO_2 at Hydrostation 'S' was estimated from monthly averaged atmospheric CO_2 data measured at La Jolla (Keeling 1993b, and unpublished), and at Bermuda (Conway et al., 1994). The atmospheric data were converted from volume fraction of dry air (ppm) to the CO_2 partial pressure in µatm by adjusting to the saturated water vapor pressure using an approximation provided by Sarmiento et al., (1992). The saturated water vapor pressure was estimated at the seawater sample temperature assuming one standard atmosphere (1.01325 bar) of pressure. The La Jolla atmospheric data are used as a proxy for the trend in atmospheric CO_2 at Hydrostation 'S' because direct measurements of atmospheric CO_2 on the island of Bermuda are not available before 1989 (Conway, 1994). Where they overlap, the two atmospheric records agree within the likely uncertainties due to monthly averaging of atmospheric CO_2 data (see Bates et al., 1998), as shown in the lower panel of Figure C.

DISCUSSION

Our time series of observations at Hydrostation 'S' documents over thirteen years of seasonal and interannual variability in inorganic carbon, as well as secular trends attributable to the rising atmospheric CO_2 concentrations resulting from the burning of fossil fuels (Keeling, 1993; Lueker and Keeling, 1994; Lueker et al., 1996; Bacastow et al., 1996; Gruber and Keeling, 1998). Considerable short-term variability in DIC and TA correlates with salinity and is owing to precipitation and evaporation occurring at the sea-surface. When the DIC data are adjusted to a constant salinity (denoted sDIC), the remaining variability is predominantly seasonal. This

seasonality, driven by a combination of biological processes, air-sea exchange of CO_2, and vertical mixing, is well documented (e.g. Keeling, 1993; Bates et al., 1996; Marchal et al., 1996; Gruber and Keeling, 1998; Gruber et al., 1998). In addition there is unmistakable interannual variability in DIC, $\delta^{13}C$ and pCO_2 (Figure B). Our discussion focuses on the secular changes and interannual variability observed in our data.

The elucidation of secular trends in DIC, $\delta^{13}C$ and pCO_2 is complicated by the seasonality of the records, interannual variability in the water mass characteristics at the site, and aliasing of the data resulting from the sampling frequency (Keeling et al., 1993; Michaels and Knapp, 1996; Bates et al., 1996; Bates et al., 1998). In contrast, the salinity normalized TA (sTA) is seasonally invariant, and with the exception of brief short-term reductions, is constant over the duration of the record with no significant secular trend. To determine the secular trends in the DIC, $\delta^{13}C$ and pCO_2 observations, each of the records were fit simultaneously to a linear function in time, representing the secular trend, and to harmonics with 6 and 12 month periods, representing the seasonal cycle (Bacastow et al., 1996). The linear trends in time are summarized in Table 2. The seasonally adjusted data and linear trends are shown in Figures D and E, respectively.

Table 2. Trends in properties of seawater measured at Hydrostation 'S' after fitting the data to 6 and 12 month harmonics, representing the seasonal cycle, and straight lines, representing the secular trends.

Measured quantity	Units	Rate of change	Standard error of rate
Temperature	$°C\ yr^{-1}$	0.022	0.015
sDIC	$\mu mol\ kg^{-1}\ yr^{-1}$	0.758	0.078
$\delta^{13}C$	$‰\ yr^{-1}$	-0.0263	0.0007
pCO_2	$\mu atm\ yr^{-1}$	1.48	0.19

The seasonally adjusted data shown in Figure D are comprised of large scale interannual variability, as well as synoptic scale inhomogenities in the water mass properties (Michaels and Knapp, 1996; Bates et al., 1998). We expect the later to be more prominent as the surface mixed layer shallows and stratifies with seasonal warming in late spring and summer. In contrast, as the

surface mixed layer deepens in late winter and early spring due to convective cooling and ventilation of the seasonal thermocline, we expect the effects of localized variability to be minimized. Seasonality in the synoptic scale variability is best seen in the pCO_2 data, shown in Figure B (bottom panel). The variability is distinctly greater in the high pCO_2 values that correspond to the warmest ocean temperatures. To minimize the effects of localized variability in our analysis of the secular trends, we considered only the data collected at times of observed minima in ocean temperature. Temperature minima occur between February and April, usually coinciding with maxima in mixed layer depth and sDIC, and minima in $\delta^{13}C$ and pCO_2 as shown in Figure B.

The sDIC data at times of annual minima in temperature tend to rise over the record period, and also show an association of higher sDIC with colder temperature (over the range 18.8 to 20.7 °C). A multiple regression analysis of these data (IMSL, 1985) in which we assumed linear variations with temperature, T_c (°C) and time, t, (expressed in years since 1900) gives a relationship which accounts for over 90% of the variability in sDIC:

$$(9) \quad sDIC = 2130.15 - 8.185 \, T_c + 0.934 \, t \qquad\qquad (R^2 = 0.92)$$

with standard errors for the coefficients of 1.017 for T_c and 0.145 for t. The time dependence of the data indicates an average increase in sDIC of 0.93 μmol kg^{-1} yr^{-1}, slightly larger than the trend of 0.76 μmol kg^{-1} yr^{-1} found by fitting harmonics and a straight line to the complete record (Table 2). The temperature dependence of sDIC can be understood by considering the development of a thermally homogeneous mixed layer, and the corresponding increase in DIC that results at the time of the observed minima in ocean temperature. The deeper the mixed layer, the lower the temperature and the higher the corresponding DIC observed at the surface.

The relationship between mixed layer temperature and sDIC is best illustrated from profile measurements of the water column. We have measured a limited number of profiles during various seasons at Hydrostation 'S', shown in Figure F. Note the profiles in temperature and sDIC observed in February, 1985 showing fairly constant values to a depth greater than 125 m. Most of our observations at Hydrostation 'S' are limited to 2 and 10 meter depths. However monthly profiles in temperature and DIC to depths of 250 m have been measured at the nearby BATS site since 1989 (Bates et al., 1996; Bates et al., 1998; data available on the Web at www.bbsr.edu). A few of these profiles are shown in figure G to illustrate changes in the seasonal thermocline, and the corresponding increase in DIC.

The sDIC data corresponding to the minima in temperature are shown with the secular trend in the upper panel of Figure H. For comparison, the sDIC data measured at BATS at times of observed maxima in mixed layer depth are shown in the lower panel, also with the secular trend. The trend in sDIC at the BATS site was evaluated by averaging the sDIC data through the mixed layer at times of minima in mixed layer temperature (and coincidentally, maxima in mixed layer depths). The indicated trend was 2.37 μmol kg^{-1} yr^{-1}, significantly greater than the trend at Hydrostation 'S'. An earlier analysis reported by Bates et al. (1996) in which DIC data were integrated over the 250 m depth interval, found a trend of 1.7 μmol kg^{-1} yr^{-1}. Comparison of the BATS record with the longer time series in sDIC from Hydrostation 'S' suggests that the difference in the trends can be attributed to an anomolously warm period with lower than average sDIC that coincided with the commencement of the BATS measurements in 1989 and 1990 (Figure H).

The δ^{13}C data at times of minima in observed temperature exhibit a pronounced secular trend and, like the sDIC data, show a correlation with temperature. By a multiple linear regression analysis similar to that used for DIC we found for δ^{13}C:

(10) $\quad \delta^{13}C = 2.1572 + 0.0639\ T_c - 0.0229\ t$ $\qquad\qquad$ $(R^2 = 0.91)$

Standard errors of the coefficients were 0.0178 for T_c and 0.0025 for t. In a similar analysis of the data through 1993, Bacastow et al. (1996) fit the complete record of $\delta^{13}C$ data to a harmonic function to represent average seasonality, a linear trend function, and a spline function proportional to a smoothed representation of the annual minimum temperature data. Correlation of the $\delta^{13}C$ data with the annual minimum temperature provides evidence that the extent of winter ventilation establishes the interannual variability in $\delta^{13}C$ throughout the year. Thus, the trend in the data at times of observed minima in temperature, -0.023 ‰ yr^{-1}, is very similar to the linear trend of -0.026 ‰ yr^{-1} found by fitting harmonics and a straight line to the complete record.

Calculated pCO$_2$ data corresponding to annual minima in temperature were also fit with a multiple linear regression analysis to temperature and time:

(11) $\quad pCO_2 = 89.56 + 3.77\ T_c + 1.55\ t$ $\qquad\qquad$ $(R^2 = 0.56)$

Standard errors of the coefficients were 2.98 for T_c and 0.424 for t. Although the correlation of pCO$_2$ with temperature was not as significant as that for DIC and $\delta^{13}C$, the secular trend in pCO$_2$ of 1.55 μatm yr^{-1} was nearly the same, as the linear trend found by fitting harmonics and a straight line to the complete record. The observed trend in pCO$_2$ also agrees, within the uncertainties in the fit, with the average increase in atmospheric CO$_2$ observed during the record of 1.40 μatm yr^{-1}. The trends in sDIC, $\delta^{13}C$ and pCO$_2$ are shown in Figure I.

Model Predictions

We compared the observed secular increases in sDIC, $\delta^{13}C$, and pCO$_2$ with predictions from a three-dimensional ocean circulation model, "HAMOCC3" (Bacastow, pers.com., 1998; Six and

Maier-Reimer, 1996) for a model grid cell of about 10^5 km^2 which includes Hydrostation 'S'.

Coincidentally, this model also predicts nearly the same increases in sDIC, δ^{13}C, and pCO$_2$

averaged over the global oceans. Thus, we also compare our observations to predictions from a

global compartment model, or "box diffusion model" (Siegenthaler, 1983; Keeling et al., 1989).

The results are summarized in Table 3.

Table 3. Comparison of observed and predicted linear trends in properties of seawater measured
at Hydrostation 'S' from 1984 to 1997.

Measured quantity	Units	Rate of change (all data)	Rate of change (annual minima in Temperature)	HAMOCC3 Near Bermuda	HAMOCC3 Global	Box Diffusion Model
SDIC	μmol kg^{-1} yr^{-1}	0.76	0.93	0.78	0.75	0.81
δ^{13}C	‰ yr^{-1}	-0.026	-0.023	-0.017	-0.017	-0.015
PCO$_2$	μatm yr^{-1}	1.48	1.55	1.30	1.39	1.36

A net flux into the ocean of CO$_2$ from fossil fuel combustion accounts for most of the secular

trends of DIC, pCO$_2$, and δ^{13}C observed in our data at times of annual temperature minima. The

pCO$_2$ the mixed-layer has an adjustment time of approximately one year with respect to changing

atmospheric CO$_2$ (Broecker and Peng, 1982). Therefore pCO$_2$ can be expected to rise at close to

the rate of increase of atmospheric CO$_2$, as is observed in our data for Hydrostation 'S'.

Furthermore, as temperature and sTA show no significant secular trends at Hydrostation "S",

sDIC rises at close to the predicted rate. In contrast, the adjustment time for δ^{13}C is on the order

of 10 years (Broecker and Peng, 1982). The trend in δ^{13}C of surface waters is therefore relatively

more sensitive to the rate of vertical mixing, especially the degree of ventilation of the upper

oceans at times of minimum temperature when this mixing is maximal. A study by Druffel (1997)

suggests that variability in ventilation near Bermuda is important for isotopic tracers of the

carbon cycle. Measurements of ^{14}C and δ^{13}C in a coral sampled near Bermuda furnish a proxy

record of the oceanic signals from 1885 to 1955, (Druffel, 1997). It is evident from the coral data

that the rate of ventilation of the upper oceans near Bermuda has varied considerably with a periodicity of 6 and 9 years. The $\delta^{13}C$ of the same coral record suggests that large-scale departures from the fossil fuel trend have persisted for intervals up to a decade.

Summary

Measurements of DIC, TA and of $\delta^{13}C$ in surface seawater establish the seasonality of the carbon cycle measured for more than 13 years at Hydrostation 'S'. The cycle involves air-sea exchange of CO_2, inorganic carbon uptake and release arising from organic processes, and the entrainment of waters from below, all occurring in a surface mixed-layer of varying thickness. The DIC and pCO_2 data show a secular increase approximately as predicted by model calculations of the net flux of CO_2 into the oceans resulting from air-sea exchange and increasing atmospheric CO_2 concentrations. The secular decrease in $\delta^{13}C$ appears to exceed the predicted decrease due to air-sea exchange. DIC, and $\delta^{13}C$ data exhibit considerable interannual variability, most of which is correlated with the depth of convective mixing in late winter or early spring, as reflected in the annual minima in observed temperature. Variability in pCO_2 is more strongly influenced by synoptic scale variability, and hence is not as strongly correlated with the annual minima in ocean temperature (Bates et al., 1998).

This time series establishes a baseline data set for interpreting the dynamics and interannual variability of inorganic carbon in nutrient-poor, subtropical near-surface ocean water. The record adds to a much longer earlier time series of basic physical and chemical measurements at the same site and should provide additional clues to the ocean's link between climate change and the global carbon cycle.

Acknowledgements

References

Anderson, L.A. and Sarmiento, J.L., 1994. Redfield ratios of remineralization determined by nutrient data analysis. Global Biogeochem. Cycles 8: 65-80.

Bacastow, R. B., 1981. Numerical evaluation of the evasion factor. In Scope 16: Carbon Cycle Modeling, edited by B. Bolin, John Wiley and Sons, Chichester, 95-101.

Bacastow, R., and Maier-Reimer, E., 1990. Ocean-circulation model of the carbon cycle. Climate Dynamics 4: 95-125.

Bacastow, R.B., Keeling, C.D., Lueker, T.J., Wahlen, M. and Mook, W., 1996. The ^{13}C Suess effect in the world surface oceans and its implications for oceanic uptake of CO_2: Analysis of observations at Bermuda. Global Biogeochem. Cycles 10: 335-346.

Bates, N. R., Michaels, A. F. and Knap, A. H., 1995. Alkalinity changes in the Sargasso Sea: geochemical evidence of calcification? Marine Chemistry 51: 347-358.

Bates, N. R., Michaels, A. F. and Knap, A. H., 1996. Seasonal and interannual variability of oceanic carbon dioxide species at the U.S. JGOFS Bermuda Atlantic Times-series Study (BATS) site. Deep-Sea Research II 43: 347-383.

Bates, N.R., Takahashi, T., Chipman, D.W., and Knap, A.H., 1998. Variability of pCO_2 on diel to seasonal timescales in the Sargasso sea near Bermuda. J. Goephys. Res., 103: (NC8) 15567-15585.

Bevington, P. R., 1969. Data Reduction and Error Analysis for the Physical Sciences. McGraw-Hill, New York, N.Y., 336 pp.

Bisset, W.P., Meyers, M.B., Walsh, J.J. and Muller-Karger, F.E. 1994. The effects of temporal variability of mixed layer depth on primary productivity around Bermuda. J.Geophys. Res., 99: 7539-7553.

Bollenbacher, A. F., C. D. Keeling, E. S. Stewart, M. Wahlen, and T. P. Whorf, 1998. Calibration methodology for the Scripps $^{13}C/^{12}C$ and $^{18}O/^{16}O$ stable isotope program, Technical Publication, Scripps Institution of Oceanography.

Bradshaw, A.L., Brewer, P.G., Shafer, D.K. and Williams, R.T., 1981. Measurements of total carbon dioxide and alkalinity by potentiometric titration in the GEOSECS program. Earth Planet. Sci. Let., 55: 99-115.

Broecker, W. S. and Peng, T.S., 1982. Tracers in the sea. Eldigio Press, Lamont-Doherty Geological Observatory, Palisades, New York. 690pp.

Conway, T. J., P. P. Tans, L. S. Waterman, and K. W. Thoning, 1994. Evidence for interannual variability of the carbon cycle from the National Oceanic and Atmospheric Administration/Climate Monitoring and Diagnostics Laboratory Global Air Sampling Network. Geophys. Res., 99: 22831-22855.

Coplen, T. B., C. Kendall, and J. Hopple 1983. Comparison of stable isotope reference samples. Nature 302: 236-238.

Craig, H., 1957. Isotopic standards for carbon and oxygen and correction factors for mass-spectrometric analysis of carbon dioxide. Geochim. Cosmochim. Acta 12: 133-149.

CRC Handbook of Chemistry and Physics, 70th Edition 1989-1990, 1990. Edited by R. C. Weast, CRC Press, Inc., Boca Raton, Florida.

Deuser, W. G., 1986. Seasonal and interannual variations in deep-water particle fluxes in the Sargasso Sea and their relation to surface hydrography. Deep-Sea Res. 33: 225-246.

Deuser, W. G., T. D. Jickells, P. King, and J. A. Commeau, 1995. Decadal and annual changes in biogenic opal and carbonate fluxes to the deep Sargasso Sea. Deep-Sea Res. I, 42: 1923-1932.

Dickson, A. G., 1981. An exact definition of total alkalinity and a procedure for the estimation of alkalinity and total inorganic carbon from titration data. Deep-Sea Res., 28A: 609-623.

Dickson, A., 1984. pH scales and proton-transfer reaction in saline media such as sea water. Geochim. Cosmochim. Acta, 48: 2299-2308.

Dickson, A. G., and F. J. Millero, 1987. A comparison of the equilibrium constants for the dissociation of carbonic acid in seawater media. Deep-Sea Res., 34: 1733-1743.

Dickson, A.D., 1992. The Determination of total dissolved inorganic carbon in sea water using extraction/coulometry: the first stage of a collaborative study. Dept. of Energy report DOE/RL/01830T-H14, 43 pp.

Dickson, A.G., Afghan, J.D. and Anderson, G.C., 1998. Sea water based reference materials for CO_2 analysis: 2. A method for the certification of total alkalinity. Submitted to Marine Chem.

DOE, 1994. Handbook of Methods for the Analysis of the Various Parameters of the Carbon Dioxide System in Sea Water, edited by A.G. Dickson and C. Goyet, Dept. of Energy, ORNL/CDIAC-74.

Doney, S.C., Glover, D.M. and Najjar, R. 1996. A new coupled, one-dimensional biological-physical model for the upper ocean: Applications to the JGOFS Bermuda Atlantic time-series study (BATS) site. Deep Sea Res. 43: 591-624.

Druffel, E. R. M., 1997. Pulses of rapid ventilation in the North Atlantic surface ocean during the past century. Science, 275: 1454-1457.

Dyrssen, D., and L. G. Sillen, 1967. Alkalinity and total carbonate in sea water. A plea for p-T independent data, Tellus, 19, 113-120.

Edmond, J.M., 1970. High precision determination of titration alkalinity and total carbon dioxide content of sea water by potentiometric titration. Deep-Sea Res., 17: 737-750.

Gordon, L.I., Jennings, J.C., Ross, A.A. and Krest, J.M., 1993. A suggested protocol for continuous flow automated analysis of seawater nutrients (phosphate, nitrate, nitrite, and silicic acid) in the WOCE hydrographic program and the Joint Global Ocean Fluxes Study. OSU Coll. Of Oc. Descriptive Chem. Oc. Grp. Tech. Rpt. 93-1. Corvallis Oregon, 55pp.

Gruber N., and C. D. Keeling, 1998. Seasonal carbon cycling in the Sargasso Sea near Bermuda. Scripps Institution of Oceanography, Bulletin vol. 30, U.C. Press, Berkeley, in press.

Gruber, N., Sarmiento, J.L. and Stocker, T.F., 1996. An improved method for detecting anthropogenic CO_2 in the oceans, Global Biogeochem. Cycles, 10, 809-837.

Gruber, N., C. D. Keeling, T. F. Stocker, 1998. Carbon-13 constraints on the seasonal inorganic carbon budget at the BATS site in the northwestern Sargasso Sea. Deep-Sea Research in press.

IMSL 1985. Library Reference Manual, ed. 9.2 (IMSL Inc., 7500 Bellair Blvd., Houston, TX 77036) Chapter R.

Jenkins, W. J., 1982. On the climate of a subtropical ocean gyre: Decade timescale variations in water mass renewal in the Sargasso Sea. J. Mar. Res., 40: 265-290.

Jenkins, W. J., and J. C. Goldman, 1985. Seasonal oxygen cycling and primary production in the Sargasso Sea. J. Mar. Res., 43: 465-491.

Joyce, T.M. and Robbins, P., 1996. The long-term hydrographic record at Bermuda. J. Climate, 9: 3121-3131.

Karl, D. M., Lukas, R. 1996 The Hawaii Ocean Time-series (HOT) program: Background, rational, and field implementation. Deep-Sea Res. II, 43, 129-156.

Keeling, C.D., Guenther, P.R., Emanuele, G.E., Lueker, T.J. and Dickson, A.G., 1998. Sea water based reference materials for CO2 analysis: 3. A method for the certification of total dissolved inorganic carbon. Submitted to Marine Chem.

Keeling, C. D., 1993a. Lecture 2: Surface ocean CO_2, in Global Carbon Cycle, edited by M. Heimann, Springer-Verlag, Berlin, 1-29.

Keeling, C. D., 1993b. Lecture 1: Global observations of atmospheric CO_2, in Global Carbon Cycle, edited by M. Heimann, Springer-Verlag, Berlin, 1-29.

Keeling, C. D., P. R. Guenther, and D. J. Moss, 1986. An analysis of the concentration of atmospheric carbon dioxide-in-air standards: Revision of 1985, Report No. 4 of the Environmental Monitoring Programme of the World Meteorological Organization, Geneva, 34 pp. and Addendum, 43 pp.

Keeling, C. D., R. B. Bacastow, A. F. Carter, S. C. Piper, T. P. Whorf, M. Heimann, W. G. Mook and H. Roeloffzen, 1989. A three-dimensional model of atmospheric CO_2 transport based on observed winds: 1. Analysis of observational data. In: Aspects of Climate Variability in the Pacific and the Western Americas, edited by D.H. Peterson, Geophysical Monograph *55*, 165-236.

Lai, D. Y., and P. L. Richardson, 1997. Distribution and movements of Gulf Stream rings. J. Phys. Oceanogr., 7: 670-683.

Laitenin, H.A., 1960. Chemical analysis: An Advanced Text and Reference. Mcgraw Hill, New York, N.Y.

Lueker, T.J. and C. D. Keeling, 1994. Inorganic carbon variations in surface ocean water at Station 'S' near Bermuda. EOS, Transactions, American Geophysical Union,75: 111.

Lueker, T.J., 1998. The ratio of the first and second dissociation constants of carbonic acid determined from the concentration of carbon dioxide in gas and seawater at equilibrium. Ph.D. Dissertation. Univ. of Cal. San Diego, San Diego, 155 pp.

Marchal, O., Monfray, P., Bates, N.R. 1996. Spring-summer imbalance of dissolved inorganic carbon in the mixed layer of the northwestern Sargasso Sea, Tellus, Ser. B., 48, 115-134.

Mehrbach, C., Culberson, C. H., Hawley, J. E., and Pytkowicz, R.M., 1973. Measurements of the apparent dissociation constants of carbonic acid in seawater at atmospheric pressure, *Limnol. Oceanogr 18*, 897-907.

Menzel, D. W., and J. H. Ryther, 1960. The annual cycle of primary production in the Sargasso Sea off Bermuda. Deep-Sea Res. 6: 351-367.

Michaels, A. F., A. H. Knap, R. L. Dow, K. Gundersen, R. J. Johnson, J. Sorensen, A. Close, G. A. Knauer, S. E. Lorenz, V. A. Asper, M. Tuel, and R. Bidigare, 1994a. Seasonal patterns of

ocean biogeochemistry at the U.S. JGOFS Bermuda Atlantic Time-series Study site. Deep-Sea Res., 41: 1013-1038.

Michaels, A. F., N. R. Bates, K. O. Buesseler, C. A. Carlson, and A. H. Knap, 1994b. Carbon-cycle imbalances in the Sargasso Sea. Nature, 372: 537-540.

Michaels, A.F., D. A. Caron, N.R. Swanberg, F.A. Howse, and C. M. Michaels. 1995. Planktonic sarcodinces (Acantharia, Radiolaria, Foraminifera) in surface waters near Bermuda: abundance, biomass and vertical flux. J. Plankton Res., 17: 131-163, 1995.

Michaels, A. F., and A. H. Knap, 1996. Overview of the U.S. JGOFS Bermuda Atlantic Time-series Study and the Hydrostation S program. Deep-Sea Res. II, 43 157-198.

Mook, W. G., and P. M. Grootes, 1973. The measuring procedure and corrections for the high-precision mass-spectrometric analysis of isotopic abundance ratios, especially referreing to carbon, oxygen and nitrogen. International Journal of Mass Spectrometry and Physics, 12: 273-298.

Mook, W. G., M. Koopmans, A. F. Carter, and C. D. Keeling, 1983. Seasonal, latitudinal, and secular variations in the abundance and isotopic ratios of atmospheric carbon dioxide, J. Geophys. Res., 88, 10915-10933.

Mook, W. G., and S. Van der Hoek, 1983. The N_2O correction in the carbon and oxygen isotopic analysis of atmospheric CO_2 . Isotope Geoscience 1: 237-242.

Oblers, D., Wenzel, M. and Willebrand, J., 1985. The inference of North Atlantic circulation patterns from climatological hydrographic data. Rev. Geophys., 23: 313–356.

Platt, T., and W. G. Harrison, 1985. Biogenic fluxes of carbon and oxygen in the ocean, Nature 318: 55-58.

Redfield, A. C., B. H. Ketchum, and F. A. Richards, 1963. The influence of organisms on the composition of sea-water. In: The Sea, edited by M. N. Hill, John Wiley & Sons, New York, 26-77.

Sambrotto, R. N., G. Savidge, C. Robinson, P. Boyd, T. Takahashi, D. M. Karl, C. Langdon, D. Chipman, J. Marra, and L. Codispoti, 1993. Elevated consumption of carbon relative to nitrogen in the surface ocean. Nature 363: 248-250.

Sarmiento, J. L., J. C. Orr, and U. Siegenthaler, 1992. A perturbation simulation of CO_2 uptake in an ocean general circulation model, J. Geophys. Res., 97, 3621-3645.

Sarmiento, J.L. and LeQuere, C., 1996. Oceanic carbon dioxide uptake in a model of century-scale global warming. Science, 274: 1346-1350.

Schroeder E., and H. Stommel, 1969. How representative is the series of Panulirus stations of monthly mean conditions off Bermuda? Progress in Oceanography, 5: 31-40.

Sengers, J. M. H., Levelt, M. Klein, and J. S. Gallagher, 1971. Pressure-Volume-Temperature Relationships of Gases-Virial Coefficients. U.S. N.B.S. Report, U.S. Air Force Technical Publication. AEDC-TR-71-39.

Siegel D. A., A. F. Michaels, J. C. Sorensen, M. C. O'Brien, and M. Hammer, 1995. Seasonal variability of light availability and its utilization in the Sargasso Sea.. J. Geophys. Res., 100: 8695-8713.

Siegenthaler, U. 1983. Uptake of excess CO_2 by an outcrop-diffusion model of the ocean. J. Geophys. Res. 88: 3599-3608.

Siegenthaler, U. and Sarmiento, J., 1993. Atmospheric carbon dioxide and the ocean. Nature 365: 119-125.

Six, K. D. and Maier-Reimer, E., 1996. Effects of plankton dynamics on seasonal carbon fluxes in an ocean general circulation model. Global Biogeochem. Cycles 10: 559-583.

Spitzer, W. S., and Jenkins, W. J., 1989. Rates of vertical mixing, gas exchange and new production: Estimates from seasonal gas cycles in the upper ocean near Bermuda. J. Mar. Res. 47: 169-196.

Takahashi, T., D. Chipman, N. Schechtman, J. Goddard, and R. Wanninkof, 1982. Measurements of the partial pressure of CO_2 in discrete water samples during the North Atlantic Expedition, the Transient Tracers of the Ocean Project, Tech. Rept. to the National Science Foundation, 268 pp., Lamont-Doherty Geol. Obs., Palisades, N.Y.

Takahashi, T., J. Olafsson, J. G. Goddard, D. W. Chipman, and S. C. Sutherland, 1993. Seasonal variation of CO_2 and nutrients in the high-latitude surface oceans: A comparative study, Global Biogeochem. Cycles, 7, 843-878.

Takahashi, T., Broecker, W.S., Langer, S., 1985. Redfield ratios based on chemical data from isopycnal surfaces. J. Geophys. Res. 90 (C4): 6907-6924.

Talley, L. D. and M. E. Raymer, 1982. Eighteen degree water variability. J. Mar. Res., 40: 757-775.

Tans, P.P., Fung, I.Y., Takahashi, T., 1990. Observational constraints on the global atmospheric CO_2 budget. Science 247, 1431-1438.

Tans, P.P., Berry, J.A., Keeling, R.F., 1993. Oceanic 13C/12C Observations: A new window on oceanic CO_2 uptake. Global Biogeochem. Cycles 7, 353-368.

Toggweiler, J. R., 1994. Vanishing in Bermuda. Nature 372: 505-506.

Tourre, Y. M. and W. B. White. 1995. ENSO signals in global upper-ocean temperature. J. Phys. Oceanogr. 25: 1317-1332.

Weiss, R.F., 1981. Determinations of carbon dioxide and methane by dual catalyst flame ionization chromatography and nitrous oxide by electron capture chromatography. J. Chromatographic Sci. 19: 611-616.

Winn, C.D., Mackenzie, F.T., Carrillo, C.J., Sabine, C.L., and Karl, D.M. 1994. Air-sea carbon dioxide exchange in the North Pacific Subtropical Gyre: Implications for the global carbon budget. Global Biogeochem. Cycles, 8, 157-163.

Winn, C. D., Li, Y., Mackenzie, F.T., Karl, D.M. 1998. Rising surface ocean dissolved inorganic carbon at the Hawaii Ocean Time-series site. Mar. Chem. 60, 33-47.

Wong, C. S., 1970. Quantitative analysis of total carbon dioxide in sea water: A new extraction method. Deep-Sea Res. 17: 9-17.

Worthington, L.V., 1976. On the North Atlantic circulation. The John Hopkins Oceanographic Studies, 6, 1-110.

Table 1. Properties of Seawater Measured at Hydrostation 'S' from 1983-1997. Pair deltas refer to the difference of two analyses that produce the mean value listed in the previous column. The pCO2 data were calculated using equations from Dickson (1998 pers. Com.), see Lueker 1998.

Sample Date	Depth	Salinity	Temp.	DIC	flag	Pair Delta	TA	flag	Pair Delta	$\delta^{13}C$	flag	Pair delta	pCO_2
12Sep83	1	36.150	28.01	1999.54	-	0.94	-	A	-	1.550	S	-	365.36
12Sep83	10	36.146	27.24	2000.52	-	0.87	-	A	-	1.540	S	-	356.26
10Oct83	1	35.956	26.35	1987.33	-	0.65	2346.18	S	-	1.615	-	0.050	339.03
10Oct83	10	35.951	26.35	1986.95	-	0.53	2346.35	S	-	1.600	S	-	338.20
27Jan84	1	36.400	20.20	2031.94	-	1.33	2369.89	S	-	1.505	-	0.010	300.89
27Jan84	10	36.381	20.41	2030.01	-	0.07	-	A	-	1.345	-	0.050	294.56
09Mar84	1	36.463	19.81	2043.46	-	0.44	-	A	-	-	A	-	300.16
09Mar84	10	36.466	19.88	2042.86	-	0.41	-	A	-	-	A	-	300.02
03Apr84	1	36.484	19.61	2046.66	-	0.45	-	A	-	1.425	-	0.010	300.75
03Apr84	10	36.468	19.49	2044.80	-	0.50	-	A	-	1.390	S	-	297.71
30Apr84	1	36.479	19.74	2043.68	-	0.22	-	A	-	1.460	-	0.020	298.64
30Apr84	10	36.481	20.05	2043.88	-	0.63	-	A	-	1.455	-	0.010	302.57
28Jun84	1	36.307	23.78	-	A	-	-	A	-	-	A	-	
28Jun84	10	36.299	23.44	2024.09	-	0.70	-	A	-	1.545	-	0.050	329.83
25Jul84	1	36.446	27.12	2033.54	-	1.57	-	A	-	-	A	-	386.33
25Jul84	10	36.442	26.65	2030.83	-	0.15	-	A	-	1.575	-	0.010	375.03
16Aug84	1	36.454	28.09	2022.67	-	1.46	-	A	-	1.570	-	0.020	381.93
16Aug84	10	36.414	27.29	2022.01	-	0.05	2369.31	S	-	1.585	-	0.010	383.22
11Sep84	1	36.497	26.69	2018.15	-	0.96	-	A	-	1.640	-	0.040	351.69
11Sep84	10	36.494	26.60	2017.38	-	0.40	-	A	-	1.620	S	-	349.00
12Sep84	1	36.459	26.64	2017.23	S	-	-	A	-	1.630	S	-	362.05
12Sep84	50	36.487	21.81	2027.36	-	0.17	-	A	-	1.725	-	0.030	301.48
12Sep84	151	36.477	18.69	2069.14	-	1.05	2381.25	-	1.18	1.315	-	0.050	323.72
12Sep84	246	36.469	18.03	2083.13	-	0.76	-	A	-	-	A	-	335.33
12Sep84	394	36.390	17.17	2094.90	-	2.96	-	A	-	1.165	-	0.030	349.16
12Sep84	574	35.950	14.89	2125.97	-	0.36	-	A	-	1.070	-	0.000	418.96
12Sep84	780	35.355	10.50	2171.51	-	1.23	-	A	-	0.845	-	0.010	558.32
12Sep84	990	35.127	7.30	2182.06	-	0.06	2322.62	S	-	0.855	-	0.010	492.34
12Sep84	1203	35.094	5.65	2170.72	-	0.10	2321.66	-	0.50	0.960	-	0.000	419.12
12Sep84	1400	35.056	4.80	2166.44	-	4.18	2315.53	-	0.59	0.955	-	0.050	404.98

Table 1   cont.

Sample Date	Depth	Salinity	Temp.	DIC	flag	Pair Delta	TA	flag	Pair Delta	δ¹³C	flag	Pair delta	pCO₂
12Sep84	1992	35.001	3.88	2158.64	-	1.19	2314.03	S	-	1.060	-	0.020	373.38
12Sep84	3000	34.938	3.19	2162.04	-	0.54	2324.88	S	-	1.095	-	0.010	344.10
12Sep84	4000	34.894	2.63	2175.67	-	0.03	2331.41	-	1.00	1.045	-	0.010	353.20
18Oct84	1	36.378	23.14	2020.00	-	1.37	-	A	-	1.615	-	0.010	314.89
18Oct84	10	36.377	23.49	2021.61	-	1.48	-	A	-	1.565	-	0.030	321.61
19Nov84	1	36.454	23.52	2023.94	-	0.65	2378.70	-	0.75	1.630	-	0.040	322.96
19Nov84	10	36.456	22.44	2023.73	-	0.17	2379.88	-	1.27	1.635	-	0.030	307.48
17Dec84	1	36.434	20.79	2030.08	-	0.76	2380.41	-	2.92	1.615	-	0.010	295.07
17Dec84	10	36.431	20.76	2029.91	-	1.04	2379.33	-	0.55	1.615	-	0.010	295.53
05Feb85	1	36.489	19.12	2048.77	-	0.87	-	A	-	1.410	-	0.000	306.18
05Feb85	10	36.508	19.21	2048.16	-	1.44	2383.19	S	-	1.455	-	0.050	297.94
12Feb85	1	36.513	19.04	2051.09	-	0.04	2383.37	-	0.88	1.415	-	0.010	299.52
12Feb85	10	36.511	18.96	2051.10	-	0.47	2385.38	S	-	1.460	-	0.000	295.65
12Feb85	46	36.508	19.13	2050.39	-	0.67	-	A	-	1.425	-	0.010	298.45
12Feb85	132	36.507	18.93	2051.06	-	0.22	-	A	-	1.460	-	0.080	296.94
12Feb85	220	36.448	0-00	2071.29	-	1.31	-	A	-	1.265	-	0.050	
12Feb85	352	36.447	17.99	2088.50	-	0.09	-	A	-	1.220	-	0.040	345.59
12Feb85	682	35.966	14.80	2124.97	-	0.63	-	A	-	1.040	-	0.020	413.36
12Feb85	776	35.812	13.72	2136.60	-	0.13	2347.21	S	-	0.970	-	0.020	422.63
12Feb85	962	35.218	9.26	2179.34	-	0.33	-	A	-	0.830	S	-	590.09
12Feb85	1145	35.103	6.61	2180.42	-	0.17	2321.96	S	-	0.835	-	0.030	461.77
12Feb85	1324	35.077	5.49	2172.14	S	-	-	A	-	0.900	S	-	507.56
12Feb85	1844	35.014	4.11	2158.09	-	2.61	2313.07	S	-	1.090	-	0.020	377.65
12Feb85	2523	34.978	3.20	2159.66	-	0.01	2318.18	-	0.39	1.095	-	0.030	355.74
12Feb85	3364	34.912	2.49	2167.86	-	0.51	2323.36	-	3.71	1.055	-	0.070	352.92
15Mar85	1	36.520	19.18	2049.63	-	1.24	2383.23	-	4.21	1.470	-	0.000	299.46
15Mar85	10	36.520	19.03	2048.77	-	0.35	2384.09	-	0.01	1.470	-	0.000	295.42
11Apr85	1	36.467	19.14	2046.46	-	0.53	2377.31	-	4.42	1.445	-	0.030	300.71
11Apr85	10	36.460	19.11	2046.70	-	0.02	2378.51	-	1.71	1.460	S	-	299.26
06May85	1	36.476	20.12	2046.33	-	1.46	2375.04	S	-	1.530	-	0.040	314.99
06May85	10	36.473	19.89	-	A	-	2376.53	S	-	1.515	-	0.010	
25Jun85	1	36.483	26.13	2036.77	-	0.33	-	A	-	-	A	-	374.10
25Jun85	10	36.475	25.76	2035.61	-	0.29	-	A	-	1.560	-	0.000	367.29

Table 1   cont.

Sample Date	Depth	Salinity	Temp.	DIC	flag	Pair Delta	TA	flag	Pair Delta	$\delta^{13}C$	flag	Pair delta	pCO_2
22Jul85	1	36.434	27.23	2026.98	-	0.21	2374.72	S	-	1.605	-	0.010	383.59
22Jul85	10	36.425	26.70	2026.26	-	0.11	-	A	-	1.560	-	0.060	369.44
26Aug85	1	36.472	27.86	2019.59	-	0.32	-	A	-	1.620	-	0.000	372.09
26Aug85	10	36.456	27.06	2017.37	-	0.68	-	A	-	1.635	-	0.030	358.22
14Oct85	1	36.348	25.76	2004.60	-	1.82	-	A	-	1.695	-	0.090	328.72
14Oct85	10	36.353	25.70	2004.98	-	0.32	2374.21	S	-	1.700	-	0.060	327.67
07Nov85	1	36.398	24.81	2016.36	-	0.64	-	A	-	1.665	-	0.030	329.95
07Nov85	10	36.402	24.89	2015.56	-	1.50	2376.79	S	-	1.630	-	0.000	329.76
05Dec85	1	36.542	22.62	2026.01	-	0.89	2384.50	-	0.19	1.680	-	0.040	308.29
05Dec85	10	36.541	22.57	2026.36	-	0.49	-	A	-	1.650	-	0.020	306.27
03Feb86	1	36.551	19.97	2039.02	-	0.06	2387.60	-	3.94	1.620	-	0.040	290.07
03Feb86	10	36.546	20.13	2039.60	-	1.63	2386.55	-	2.15	1.580	-	0.020	294.30
05Apr86	1	36.435	20.10	2040.61	-	0.67	-	A	-	1.510	-	0.000	301.66
05Apr86	10	36.440	20.00	2038.80	-	2.83	2381.39	-	4.94	1.475	-	0.030	295.58
28Apr86	1	36.535	20.02	2042.08	-	0.02	-	A	-	1.540	-	0.040	296.43
28Apr86	10	36.535	20.35	2041.11	-	0.18	-	A	-	1.480	-	0.000	299.14
29May86	2	36.583	21.42	2041.81	-	0.55	2388.64	-	4.51	1.550	-	0.000	310.51
29May86	12	36.580	21.77	2041.02	-	1.26	2390.01	-	1.27	1.550	-	0.000	312.25
07Jul86	1	36.323	25.99	2021.28	-	1.25	2375.30	-	0.77	1.570	-	0.020	355.48
07Jul86	10	36.371	26.00	2024.42	-	1.01	2374.65	-	0.53	1.595	-	0.030	361.21
26Aug86	1	36.384	27.90	2014.79	-	0.31	2375.86	-	0.19	1.670	S	-	371.62
26Aug86	10	36.379	27.74	2014.51	-	0.30	2376.99	-	0.09	1.655	-	0.010	367.05
23Sep86	1	36.213	26.31	2000.33	-	0.41	2364.66	-	0.86	1.660	-	0.020	338.55
23Sep86	10	36.207	25.95	2000.19	-	0.46	2364.15	-	0.01	1.625	-	0.050	334.09
05Nov86	1	36.549	24.28	2018.55	-	0.02	2386.48	-	0.62	1.695	-	0.050	316.69
05Nov86	10	36.555	24.07	2018.34	-	0.27	2385.95	-	1.03	1.675	-	0.030	314.37
21Nov86	1	36.530	23.49	2019.21	-	2.05	2382.34	-	2.02	1.590	-	0.020	311.80
21Nov86	10	36.530	23.48	2020.61	-	0.77	2380.60	-	4.49	1.590	S	-	315.51
22Jan87	1	36.514	20.58	2040.53	S	-	2384.64	S	-	1.470	S	-	302.09
22Jan87	10	36.508	20.47	-	A	-	2386.89	-	3.18	1.465	-	0.010	
07Mar87	1	36.623	19.28	2053.76	-	1.94	2392.85	S	-	1.440	-	0.080	296.00
07Mar87	10	36.621	19.26	2053.85	-	0.90	2393.80	-	3.57	1.420	-	0.040	294.86
28Mar87	1	36.570	19.24	2054.53	-	1.01	2388.75	-	2.28	1.400	-	0.020	300.79

Table 1   cont.

Sample Date	Depth	Salinity	Temp.	DIC	flag	Pair Delta	TA	flag	Pair Delta	$\delta^{13}C$	flag	Pair delta	pCO_2
28Mar87	10	36.565	18.87	2054.16	-	1.31	2389.19	-	0.96	1.400	-	0.040	295.02
22Apr87	1	36.641	20.27	2051.40	-	0.36	2393.51	-	2.06	1.475	-	0.030	304.67
22Apr87	10	36.640	20.18	2049.97	-	0.34	2392.54	-	0.00	1.470	-	0.000	302.40
26May87	1	36.498	22.51	2035.02	-	1.60	2383.41	-	1.46	1.530	-	0.000	320.46
26May87	10	36.523	22.13	2037.59	-	0.19	2384.19	-	0.11	1.620	-	0.040	318.47
26Jun87	1	36.504	25.59	2028.34	-	0.28	2384.53	-	0.03	1.580	-	0.060	350.42
26Jun87	10	36.500	24.96	2029.21	-	0.63	2384.73	-	1.58	1.570	-	0.020	343.48
18Jul87	1	36.528	27.19	2025.64	-	0.40	2386.11	-	1.53	1.520	-	0.020	367.21
18Jul87	10	36.520	27.19	2025.90	-	0.79	2385.73	-	0.77	1.520	-	0.020	368.00
27Aug87	1	36.454	25.95	2020.37	-	0.58	2378.34	-	0.37	1.560	-	0.000	350.34
27Aug87	10	36.449	25.70	2020.36	-	0.31	2378.89	-	4.09	1.580	-	0.080	346.10
19Oct87	1	35.959	26.03	1984.09	-	1.32	2338.70	-	0.56	1.570	-	0.060	339.27
19Oct87	10	36.215	26.04	1997.76	-	0.30	2353.94	-	0.15	1.575	-	0.010	344.44
11Nov87	1	36.428	24.33	2015.83	-	1.66	2377.00	-	0.93	1.560	-	0.020	323.14
11Nov87	10	36.424	24.27	2016.20	-	0.47	2376.52	-	1.02	1.610	-	0.020	323.32
03Dec87	1	36.514	22.14	2027.80	-	0.87	2384.29	S	-	1.495	-	0.010	304.84
03Dec87	10	36.510	22.11	2027.44	-	0.81	2384.15	-	0.41	1.530	-	0.000	304.03
25Jan88	1	36.492	19.79	2042.96	-	0.29	2383.99	-	1.56	-	A	-	296.44
25Jan88	10	36.493	19.78	2042.70	-	0.29	2381.53	-	0.72	1.340	-	0.000	298.59
09Mar88	1	36.537	19.09	2050.78	-	0.44	2387.01	-	2.22	1.315	-	0.010	298.11
09Mar88	10	36.535	18.99	2050.34	-	0.49	2386.23	-	0.30	1.335	-	0.010	294.61
12May88	1	36.532	20.58	2041.72	-	0.05	2377.08	-	0.33	1.390	-	0.060	312.47
12May88	10	36.520	20.24	2041.30	-	0.25	2373.79	-	0.11	1.375	-	0.010	311.31
13Jun88	1	36.512	23.29	2040.03	-	0.94	2385.45	-	3.08	1.450	-	0.000	335.77
13Jun88	10	36.507	23.27	2039.52	-	0.49	2384.33	-	0.43	1.430	S	-	335.95
21Jul88	1	36.279	26.93	2020.78	-	0.76	2369.48	-	1.87	1.455	-	0.050	374.34
21Jul88	10	36.281	26.29	2021.26	-	1.07	2370.92	-	0.44	1.420	-	0.020	363.92
24Aug88	1	36.360	28.26	2009.36	-	0.22	2374.30	-	1.61	-	A	-	369.62
24Aug88	10	36.356	28.07	2009.06	-	1.09	2373.14	-	1.10	-	A	-	367.81
20Sep88	1	36.357	27.88	2001.05	-	0.05	2372.64	-	0.26	1.570	-	0.000	353.08
20Sep88	10	36.355	27.81	1999.60	-	0.02	2373.28	-	1.38	1.620	S	-	349.11
17Nov88	1	36.381	23.52	2016.65	-	1.75	2379.39	-	0.23	1.545	-	0.030	310.68
17Nov88	10	36.384	23.43	2016.48	-	1.07	2377.74	-	0.18	1.440	S	-	311.11

Table 1   cont.

Sample Date	Depth	Salinity	Temp.	DIC	flag	Pair Delta	TA	flag	Pair Delta	$\delta^{13}C$	flag	Pair delta	pCO_2
26Apr89	1	36.618	20.54	2050.43	-	0.62	2390.08	-	1.21	1.360	S	-	310.22
26Apr89	10	36.611	20.40	2049.05	-	0.11	2390.64	-	2.32	1.385	-	0.050	305.86
22May89	1	36.573	22.69	2042.53	-	0.40	2377.27	-	1.33	1.360	S	-	341.72
22May89	10	36.580	22.34	2041.10	-	0.01	2376.43	-	1.31	1.380	S	-	335.80
21Jul89	1	36.612	27.35	2036.94	-	1.01	2390.20	-	1.64	1.510	-	0.040	383.51
21Jul89	10	36.600	26.86	2037.11	-	0.69	2393.17	-	3.54	1.540	-	0.020	372.50
01Sep89	1	36.428	27.08	2018.74	-	1.23	2380.89	-	0.72	1.570	S	-	360.33
01Sep89	10	36.457	26.93	2020.73	-	2.13	2384.67	S	-	1.565	-	0.010	356.74
28Nov89	2	36.535	22.77	2029.92	-	0.95	2386.52	S	-	1.605	-	0.010	313.30
28Nov89	10	36.527	22.76	2029.53	-	0.68	2391.55	-	0.86	1.535	-	0.010	307.06
08Jan90	3	36.761	21.58	2045.13	-	1.10	2407.32	-	1.53	1.490	S	-	298.74
08Jan90	10	36.761	21.58	2045.04	-	1.24	2403.05	-	2.17	1.435	-	0.090	303.05
24Jan90	1	36.769	21.54	2045.93	-	0.28	2400.63	-	0.47	1.475	-	0.030	306.59
24Jan90	10	36.766	21.47	2044.78	-	0.04	2400.79	-	1.67	1.490	S	-	303.84
23Feb90	2	36.743	20.86	2051.02	-	0.33	2397.96	-	2.91	1.405	-	0.010	307.55
23Feb90	10	36.742	20.84	2051.09	-	0.26	2401.84	-	1.43	1.410	-	0.020	303.23
03Apr90	1	36.777	20.72	2053.70	-	1.20	2399.45	S	-	1.430	-	0.000	308.02
03Apr90	10	36.777	20.69	2054.42	-	1.52	2398.00	-	1.44	1.460	-	0.060	310.37
10May90	2	36.825	21.16	2056.18	-	0.80	2403.32	-	2.30	1.435	-	0.050	313.19
10May90	9	36.825	21.16	2056.22	-	0.78	2403.46	-	0.06	1.410	-	0.080	313.02
07Jun90	2	36.628	23.48	2046.57	-	1.08	2384.66	-	0.61	1.465	-	0.070	350.86
07Jun90	10	36.696	23.03	2048.47	-	0.74	2388.34	-	1.47	1.475	-	0.030	343.48
12Jul90	1	36.415	26.71	2024.49	-	0.75	2363.17	-	1.88	1.460	-	0.000	387.06
12Jul90	9	36.701	26.53	2047.78	-	0.06	2390.50	-	2.47	1.510	S	-	390.91
06Aug90	1	36.462	27.18	2028.57	-	1.39	2371.43	-	1.26	1.470	S	-	391.26
06Aug90	11	36.461	26.83	2028.06	-	0.49	2375.58	-	2.54	1.495	-	0.050	379.17
03Sep90	3	36.369	27.92	2010.21	-	0.25	-	A	-	1.529	-	0.015	366.53
03Sep90	11	36.408	27.87	2013.71	-	1.00	-	A	-	1.463	-	0.003	369.42
22Oct90	2	36.664	25.55	2025.75	-	1.84	2387.02	-	1.06	1.605	-	0.010	344.85
22Oct90	10	36.664	25.55	2025.21	-	1.91	2389.34	-	2.93	1.560	-	0.000	341.25
22Oct90	24	36.666	25.55	2024.69	-	1.04	2387.42	-	0.45	1.585	-	0.010	342.72
22Oct90	51	36.676	25.54	2024.73	-	0.14	2388.26	-	2.40	1.550	-	0.060	341.70
22Oct90	77	36.667	20.96	2050.48	-	0.37	2390.76	-	2.23	1.435	-	0.030	316.38

Table 1   cont.

Sample Date	Depth	Salinity	Temp.	DIC	flag	Pair Delta	TA	flag	Pair Delta	$\delta^{13}C$	flag	Pair delta	pCO$_2$
22Oct90	104	36.648	20.00	2062.58	-	0.55	2387.45	-	1.91	1.320	S	-	324.71
22Oct90	149	36.610	19.09	2073.34	-	0.76	2388.48	S	-	1.275	-	0.010	327.05
22Oct90	197	36.583	18.69	2081.09	-	6.69	2383.74	-	1.33	1.215	-	0.030	339.48
22Oct90	251	36.537	18.44	2080.84	S	-	2384.66	S	-	-	A	-	333.21
22Oct90	300	36.521	18.17	2083.72	-	1.88	2376.98	-	0.86	-	A	-	345.45
22Oct90	353	36.465	17.90	2092.69	-	9.29	2365.88	S	-	1.210	-	0.020	372.79
22Oct90	500	36.215	16.43	2106.09	S	-	2363.22	S	-	1.110	S	-	375.27
22Oct90	702	35.676	12.82	2148.73	-	0.97	2333.84	-	7.60	0.950	-	0.060	467.26
22Oct90	1003	35.114	7.11	2181.85	-	1.72	2315.75	-	0.25	-	A	-	497.65
22Oct90	2002	35.003	3.88	2157.86	-	2.63	2309.77	-	0.08	1.105	-	0.050	379.84
22Oct90	2599	34.969	3.23	2160.45	-	2.31	2315.60	-	1.05	1.110	S	-	363.13
21Nov90	6	36.768	23.60	2030.35	-	1.40	-	A	-	1.541	-	0.002	311.55
21Nov90	12	36.773	23.61	2030.88	-	0.55	2401.70	-	1.74	1.530	-	0.033	311.85
12Dec90	3	36.654	21.89	2041.08	-	0.61	2395.07	-	4.85	1.464	-	0.013	310.06
12Dec90	10	36.644	21.90	2041.54	-	0.01	2392.65	-	1.07	1.468	-	0.003	313.09
07Jan91	1	36.743	21.75	2043.83	-	0.24	2399.36	-	1.74	1.460	-	0.019	307.62
07Jan91	9	36.749	21.70	2042.68	S	-	2402.11	S	-	1.450	S	-	303.09
20Feb91	1	36.707	20.31	2054.11	-	0.68	2393.19	-	1.05	1.370	-	0.009	310.39
20Feb91	9	36.700	20.30	2054.40	-	0.56	2391.40	S	-	1.356	-	0.007	312.66
22Mar91	1	36.719	19.97	2060.11	-	1.78	2391.41	S	-	1.344	-	0.018	316.80
22Mar91	9	36.718	19.98	2058.49	-	0.02	2393.01	-	1.23	1.319	-	0.022	312.78
08Apr91	1	36.686	19.80	2058.28	-	0.17	2383.23	-	2.68	1.322	-	0.005	321.18
08Apr91	9	36.677	19.64	2059.19	S	-	-	A	-	1.337	S	-	305.97
08May91	1	36.655	21.28	2054.57	-	0.14	2382.79	S	-	1.363	-	0.011	335.58
08May91	11	36.665	20.38	2054.82	-	0.64	2385.60	-	2.40	1.360	-	0.018	320.60
10Jun91	3	36.487	23.86	2040.67	-	0.37	2377.85	S	-	1.387	S	-	354.44
10Jun91	10	36.487	23.62	2040.91	-	1.47	2375.04	-	1.05	1.386	S	-	354.89
17Jul91	2	36.554	26.67	2035.39	-	0.53	2387.22	-	0.59	1.412	-	0.005	374.94
17Jul91	10	36.553	26.66	2036.58	-	0.04	2387.53	S	-	1.417	-	0.050	376.53
14Aug91	1	36.689	28.81	2032.32	-	0.10	2392.03	-	1.48	1.446	-	0.014	396.89
14Aug91	12	36.694	28.75	2034.43	-	0.53	2389.39	-	3.65	1.451	-	0.010	403.50
18Sep91	1	36.511	25.96	2025.41	-	0.68	2380.68	-	3.13	1.469	-	0.007	356.73
18Sep91	10	36.526	25.90	2026.54	-	0.09	2385.09	-	0.72	1.443	-	0.043	351.88

Table 1 cont.

Sample Date	Depth	Salinity	Temp.	DIC	flag	Pair Delta	TA	flag	Pair Delta	δ¹³C	flag	Pair delta	pCO₂
12Dec91	1	36.667	22.09	2041.52	-	1.50	-	A	-	1.419	-	0.009	314.83
12Dec91	9	36.666	22.09	2041.18	-	0.44	2397.71	S	-	1.432	-	0.001	309.99
13Jan92	2	36.666	20.19	2055.32	-	0.53	2394.06	-	0.57	1.332	-	0.021	309.20
13Jan92	10	36.665	20.13	2055.57	-	0.06	2394.27	-	0.17	1.344	-	0.002	308.72
17Feb92	3	36.663	19.15	2064.89	-	0.84	2386.89	-	3.64	1.262	-	0.010	317.74
17Feb92	9	36.663	19.07	2064.72	-	2.19	2385.98	-	5.25	1.254	-	0.020	317.32
12Mar92	2	36.689	19.22	2066.24	-	1.05	2388.21	S	-	1.269	-	0.005	318.92
12Mar92	10	36.680	19.08	2065.07	-	0.46	2388.67	S	-	1.270	-	0.001	314.77
18Jun92	3	36.500	23.66	2042.95	-	1.09	2380.62	-	0.42	1.304	-	0.003	352.04
18Jun92	9	36.508	23.65	2043.73	-	0.97	2379.23	-	1.82	1.287	-	0.030	354.55
15Jul92	1	36.385	26.55	2025.48	-	0.15	2374.60	-	1.84	1.406	-	0.026	371.80
15Jul92	9	36.410	26.16	2024.10	-	0.39	2378.06	-	0.91	1.402	-	0.002	359.69
19Aug92	1	36.502	29.54	2023.86	-	1.37	2380.24	-	4.28	1.362	-	0.023	407.74
19Aug92	10	36.461	28.24	2019.71	-	1.55	2380.86	-	2.87	1.389	-	0.000	379.14
16Sep92	1	35.847	27.13	1981.39	-	0.05	2342.82	-	1.51	1.495	-	0.005	344.40
16Sep92	10	36.221	27.06	2002.48	-	0.53	2367.84	-	0.61	1.488	-	0.015	349.18
14Jan93	1	36.652	20.98	2046.36	-	0.14	2392.20	-	1.35	1.318	-	0.015	308.77
14Jan93	11	36.641	20.98	2048.65	-	1.37	2395.39	-	0.11	1.270	-	0.002	308.09
10Feb93	3	36.627	19.63	2055.00	-	4.14	2396.09	-	0.14	1.291	-	0.014	299.39
10Feb93	10	36.618	19.63	2055.42	-	0.55	2392.96	-	1.25	1.283	-	0.029	302.81
17Apr93	4	36.730	20.39	2059.19	-	1.23	2399.51	-	3.07	1.267	-	0.022	311.24
17Apr93	10	36.718	20.39	2058.89	-	1.02	2400.78	-	0.28	1.262	-	0.007	309.53
11May93	4	36.592	20.66	2051.91	-	2.44	2390.12	-	0.76	1.314	-	0.021	314.27
11May93	10	36.597	20.67	2052.33	-	5.55	2390.80	-	1.34	1.321	-	0.026	314.07
11Jun93	2	36.704	23.80	2055.13	-	1.18	2384.96	-	1.71	1.293	-	0.005	369.98
11Jun93	11	36.709	23.39	2054.37	-	0.32	2386.52	S	-	1.299	-	0.019	360.46
27Jul93	2	36.430	26.15	2036.03	-	1.98	2376.86	-	1.41	1.286	-	0.032	380.50
27Jul93	10	36.426	26.13	2036.27	-	1.35	2373.76	-	3.08	1.282	-	0.014	385.21
17Aug93	2	36.773	27.73	2036.28	-	0.08	2399.46	-	2.25	1.350	-	0.012	378.29
17Aug93	10	36.659	27.62	2036.72	-	0.17	2397.05	-	1.07	1.335	-	0.001	379.73
15Sep93	2	36.401	26.99	2015.68	-	0.36	2376.49	-	4.38	1.394	-	0.013	360.27
15Sep93	10	36.394	26.99	2015.99	-	0.94	2373.93	-	2.71	1.379	-	0.005	364.14
13Oct93	1	36.414	26.07	2016.53	-	1.81	2369.99	-	5.28	1.383	-	0.011	358.90

Table 1   cont.

Sample Date	Depth	Salinity	Temp.	DIC	flag	Pair Delta	TA	flag	Pair Delta	$\delta^{13}C$	flag	Pair delta	pCO_2
13Oct93	10	36.408	26.07	2014.86	-	1.70	2370.46	S	-	1.391	-	0.026	354.29
10Nov93	2	36.656	24.60	2026.83	-	3.01	2384.64	-	2.58	1.410	-	0.009	337.36
10Nov93	9	36.546	24.60	2028.74	S	-	2387.02	S	-	1.492	S	-	336.01
08Dec93	2	36.419	23.28	2023.84	-	1.16	2378.50	-	5.91	1.395	-	0.014	320.23
08Dec93	10	36.418	23.29	2023.98	-	0.57	2381.79	-	0.33	1.415	-	0.014	316.91
13Jan94	2	36.518	20.61	2048.26	-	0.95	2386.46	-	1.85	1.274	-	0.002	312.56
13Jan94	10	36.525	20.61	2048.48	-	0.91	2389.63	-	4.51	1.301	-	0.018	309.27
16Feb94	0	36.638	20.91	2046.45	-	0.66	2392.86	-	4.04	1.315	-	0.016	307.47
16Feb94	10	36.637	20.91	2047.05	-	0.93	2395.15	-	4.48	1.303	-	0.006	305.75
21Mar94	2	36.637	19.72	2054.72	-	0.09	2395.48	-	1.05	1.233	-	0.012	300.99
21Mar94	11	36.633	19.72	2054.79	-	0.34	2393.52	-	0.86	1.245	-	0.018	303.08
20Apr94	1	36.768	21.32	2054.18	-	1.14	2402.91	-	0.18	1.358	-	0.004	313.26
20Apr94	10	36.768	21.32	2053.55	-	0.01	2403.72	-	1.51	1.361	-	0.001	311.41
18May94	2	36.559	22.51	2051.17	S	-	2390.34	S	-	1.331	S	-	337.15
18May94	11	36.562	22.51	2052.22	-	0.67	2388.88	-	2.30	1.328	-	0.002	340.62
30Jun94	1	36.426	27.58	2033.99	-	0.51	2380.98	-	1.59	1.351	-	0.002	393.35
30Jun94	10	36.400	26.12	2034.14	-	0.60	2376.36	-	0.03	1.341	-	0.004	377.55
20Jul94	11	36.521	27.41	2032.78	-	1.16	2386.75	-	0.27	1.364	-	0.011	381.86
18Aug94	2	36.395	28.56	2021.61	-	0.92	2376.83	-	4.26	1.344	-	0.036	392.99
18Aug94	9	36.390	28.34	2022.51	S	-	2376.70	-	1.74	1.385	S	-	390.86
21Sep94	2	36.542	27.29	2015.70	-	1.36	2385.89	S	-	1.436	-	0.006	353.75
21Sep94	11	36.543	27.29	2016.13	-	0.06	2387.99	-	2.60	1.439	-	0.003	351.82
21Oct94	2	36.545	23.59	2031.94	-	1.61	2389.83	-	0.64	1.400	-	0.004	323.55
21Oct94	12	36.540	23.59	2031.18	-	0.84	2388.90	-	0.71	1.444	-	0.019	324.51
16Nov94	2	36.679	22.70	2038.96	-	0.10	2397.68	-	0.01	1.398	-	0.035	314.41
16Nov94	10	36.674	22.79	2038.43	-	0.68	2399.09	-	0.88	1.378	-	0.006	312.95
11Dec94	2	36.675	22.21	2040.70	-	0.48	2394.25	-	1.02	1.386	-	0.020	314.12
11Dec94	10	36.674	22.21	2040.97	-	0.47	2396.87	-	2.72	1.377	-	0.002	311.60
12Jan95	3	36.653	20.33	2051.93	-	0.45	2395.41	-	0.17	1.286	-	0.040	304.48
12Jan95	11	36.652	20.31	2052.52	-	0.08	2395.18	S	-	1.283	-	0.033	305.15
15Feb95	2	36.618	19.12	2065.46	-	0.99	2391.99	-	0.48	1.194	-	0.001	312.03
15Feb95	11	36.618	19.13	2066.18	S	-	2393.15	-	1.06	1.215	S	-	311.55
17Mar95	3	36.601	18.94	2065.05	-	1.93	2392.20	-	1.15	1.195	-	0.032	308.33

Table 1   cont.

Sample Date	Depth	Salinity	Temp.	DIC	flag	Pair Delta	TA	flag	Pair Delta	$\delta^{13}C$	flag	Pair delta	pCO_2
17Mar95	11	36.604	18.94	2065.43	-	0.05	2395.32	-	2.04	1.188	-	0.014	305.44
12Apr95	3	36.626	18.98	2064.88	-	0.54	2395.59	-	0.38	1.240	-	0.028	305.48
12Apr95	9	36.633	18.98	2065.88	S	-	2395.18	-	0.77	1.191	S	-	307.26
12May95	2	36.831	19.35	2063.98	-	0.29	2396.30	-	1.94	1.262	-	0.035	314.82
12May95	11	36.831	19.33	2063.35	S	-	2396.28	-	0.62	1.267	S	-	313.70
14Jun95	2	36.421	24.18	2045.23	-	0.56	2382.54	-	1.37	1.256	-	0.005	359.17
14Jun95	9	36.456	24.04	2045.81	-	0.97	2384.24	-	1.23	1.258	-	0.039	356.58
13Jul95	3	36.233	27.45	2022.71	-	3.21	2369.53	-	1.66	1.259	-	0.038	385.76
13Jul95	9	36.278	27.31	2023.83	-	1.85	2372.95	-	0.51	1.275	-	0.030	381.16
22Aug95	2	36.543	25.61	2037.14	-	1.05	2388.41	-	0.37	1.310	-	0.015	359.63
22Aug95	11	36.543	25.10	2036.36	-	0.55	2389.29	-	0.75	1.306	-	0.011	350.11
14Sep95	2	36.572	27.00	2031.17	-	0.17	2392.64	-	1.13	1.384	-	0.019	365.82
14Sep95	11	36.563	26.98	2029.77	S	-	2394.34	-	4.95	1.415	S	-	361.87
11Oct95	3	36.612	26.69	2034.05	-	1.78	2395.00	-	0.88	1.363	-	0.010	363.79
11Oct95	12	36.623	26.65	2036.41	-	2.61	2394.63	-	1.18	1.371	-	0.006	367.42
12Nov95	3	36.485	24.16	2028.86	-	0.53	2385.73	-	0.35	1.371	S	-	330.78
12Nov95	10	36.483	24.16	2029.57	-	0.63	2385.73	-	0.71	1.341	-	0.023	331.66
31Jan96	4	36.636	19.42	2061.31	S	-	2397.57	-	2.47	-	A	-	304.41
31Jan96	10	36.644	19.44	2061.83	-	0.58	2396.79	-	2.83	1.186	-	0.020	305.33
14Feb96	3	36.644	18.96	2067.57	-	0.03	2397.87	-	1.94	-	A	-	306.98
14Feb96	10	36.638	18.93	2066.94	-	0.32	2397.67	-	2.30	1.153	-	0.016	305.34
14Mar96	3	36.661	19.19	2069.33	-	2.39	2400.65	-	6.80	-	A	-	308.73
14Mar96	9	36.660	19.20	2068.52	-	1.37	2398.56	-	0.74	1.146	-	0.014	309.88
13Apr96	4	36.637	18.72	2070.82	-	1.29	2396.59	-	3.07	-	A	-	309.31
13Apr96	10	36.637	18.71	2071.16	-	0.75	2395.53	-	3.81	1.148	-	0.028	310.71
08May96	4	36.668	20.55	2064.01	-	0.54	2398.12	-	1.44	-	A	-	321.67
08May96	9	36.671	20.54	2062.99	-	0.30	2398.84	-	1.35	1.201	-	0.010	319.57
12Jun96	2	36.512	24.83	2042.37	-	0.88	2386.95	-	0.08	-	A	-	359.03
12Jun96	11	36.505	24.60	2041.61	-	0.30	2386.25	-	1.27	1.226	-	0.002	355.33
10Jul96	2	36.432	26.46	2024.58	-	0.36	2388.28	-	19.76	-	A	-	351.51
10Jul96	10	36.576	26.42	2030.68	-	9.74	2378.95	-	2.35	1.247	-	0.113	374.35
08Aug96	3	36.536	27.72	2034.36	-	2.05	2384.87	-	5.06	-	A	-	396.43
08Aug96	10	36.577	27.30	2033.92	-	0.18	2383.20	-	1.56	1.287	-	0.008	387.14

Table 1   cont.

Sample Date	Depth	Salinity	Temp.	DIC	flag	Pair Delta	TA	flag	Pair Delta	δ¹³C	flag	Pair delta	pCO₂
04Sep96	1	36.484	27.74	2028.97	-	6.93	2384.36	-	2.17	-	A	-	382.11
04Sep96	10	36.483	27.74	2026.35	-	2.72	2381.86	-	1.75	1.329	-	0.015	381.04
11Oct96	1	36.598	26.63	2025.75	-	0.36	2388.43	-	1.14	-	A	-	357.24
11Oct96	10	36.601	26.50	2026.16	-	1.26	2387.66	-	1.72	1.312	-	0.006	356.99
07Nov96	1	36.601	24.10	2030.74	-	0.39	2390.44	S	-	-	A	-	327.36
07Nov96	10	36.600	24.12	2029.26	-	1.87	2392.72	-	0.79	1.334	-	0.003	322.92
13Dec96	1	36.672	21.11	2059.44	-	2.53	2388.69	-	2.33	-	A	-	333.21
13Dec96	10	36.671	21.11	2054.27	-	3.29	2390.93	-	1.98	1.234	-	0.059	322.91
15Jan97	1	36.774	20.41	2066.07	-	3.31	2397.10	-	2.27	-	A	-	324.45
15Jan97	10	36.773	20.41	2065.16	-	1.84	2397.66	-	3.20	1.185	-	0.010	322.35
29Jan97	1	36.716	19.71	2072.68	-	4.62	2391.27	-	2.05	-	A	-	331.62
29Jan97	10	36.721	19.71	2068.83	S	-	2392.50	-	3.61	1.140	S	-	324.52
10Feb97	1	36.671	19.92	2067.62	-	0.74	2386.57	-	4.23	-	A	-	332.25
10Feb97	10	36.652	19.80	2066.95	-	0.23	2386.65	-	0.10	1.163	-	0.003	328.73
19Feb97	1	36.644	19.49	2071.47	-	2.73	2382.93	-	3.04	-	A	-	336.45
19Feb97	10	36.633	19.36	2065.77	-	0.31	2384.52	-	1.62	1.156	-	0.033	324.03
06Mar97	1	36.858	20.81	2065.85	-	0.32	2399.52	-	4.46	-	A	-	327.61
06Mar97	10	36.859	20.81	2069.44	-	6.00	2400.82	-	1.46	1.215	-	0.022	330.62

Flags: Flag A indicates data which are unavailable due to sample contamination or measurement error. Flag S indicates data that represent a single analysis result.
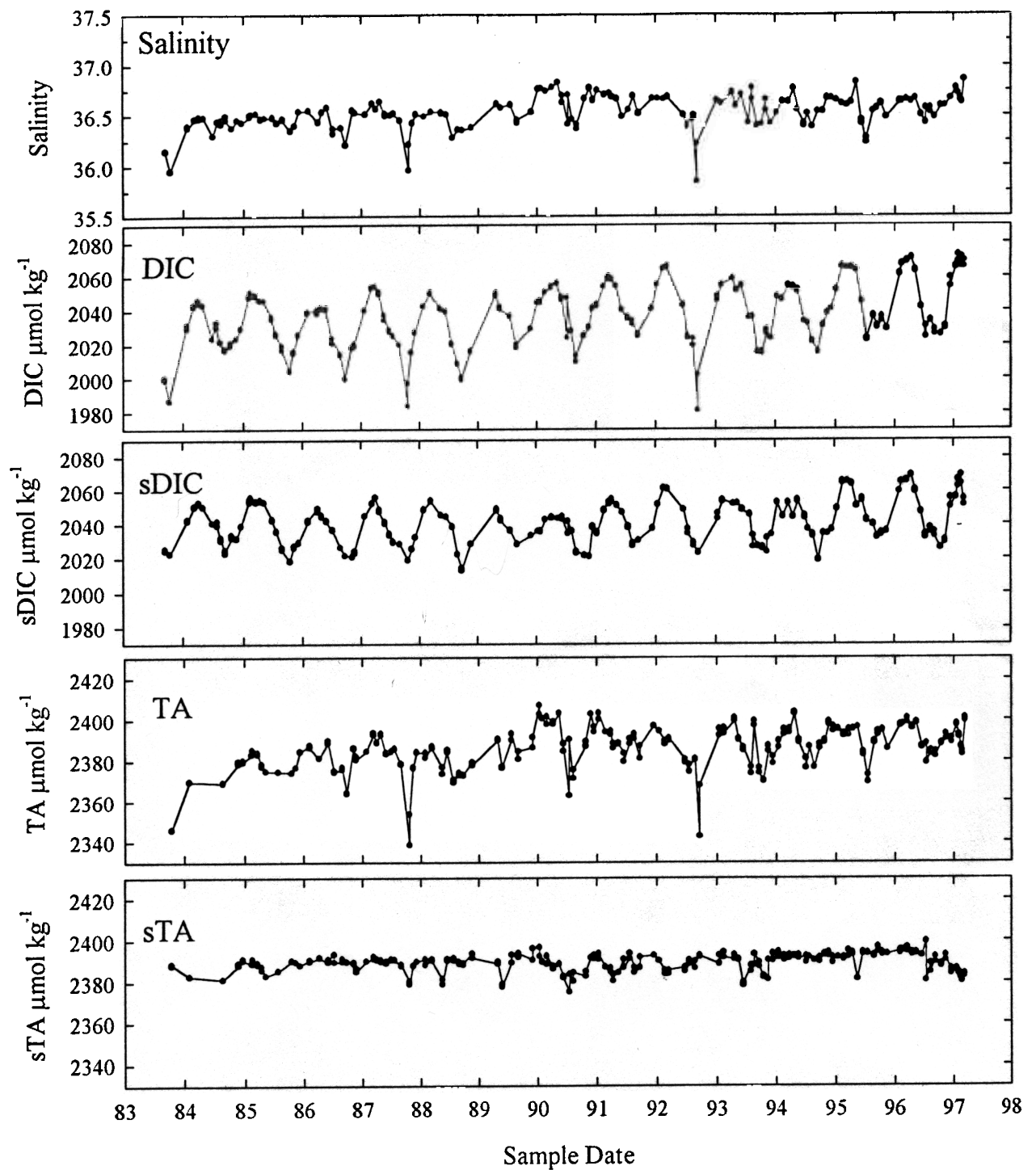
Figure A. The salinity of the seawater collected at Hydrostation 'S' is shown in the top panel. The variability in DIC attributed to changes in sample salinity is illustrated by comparing the DIC data, shown in the second panel, to the salinity normalized data (sDIC) shown in the third panel. The TA data and sTA data are also shown in the forth and bottom panels, respectively. The sDIC and sTA data were normalized to a salinity of 36.6.
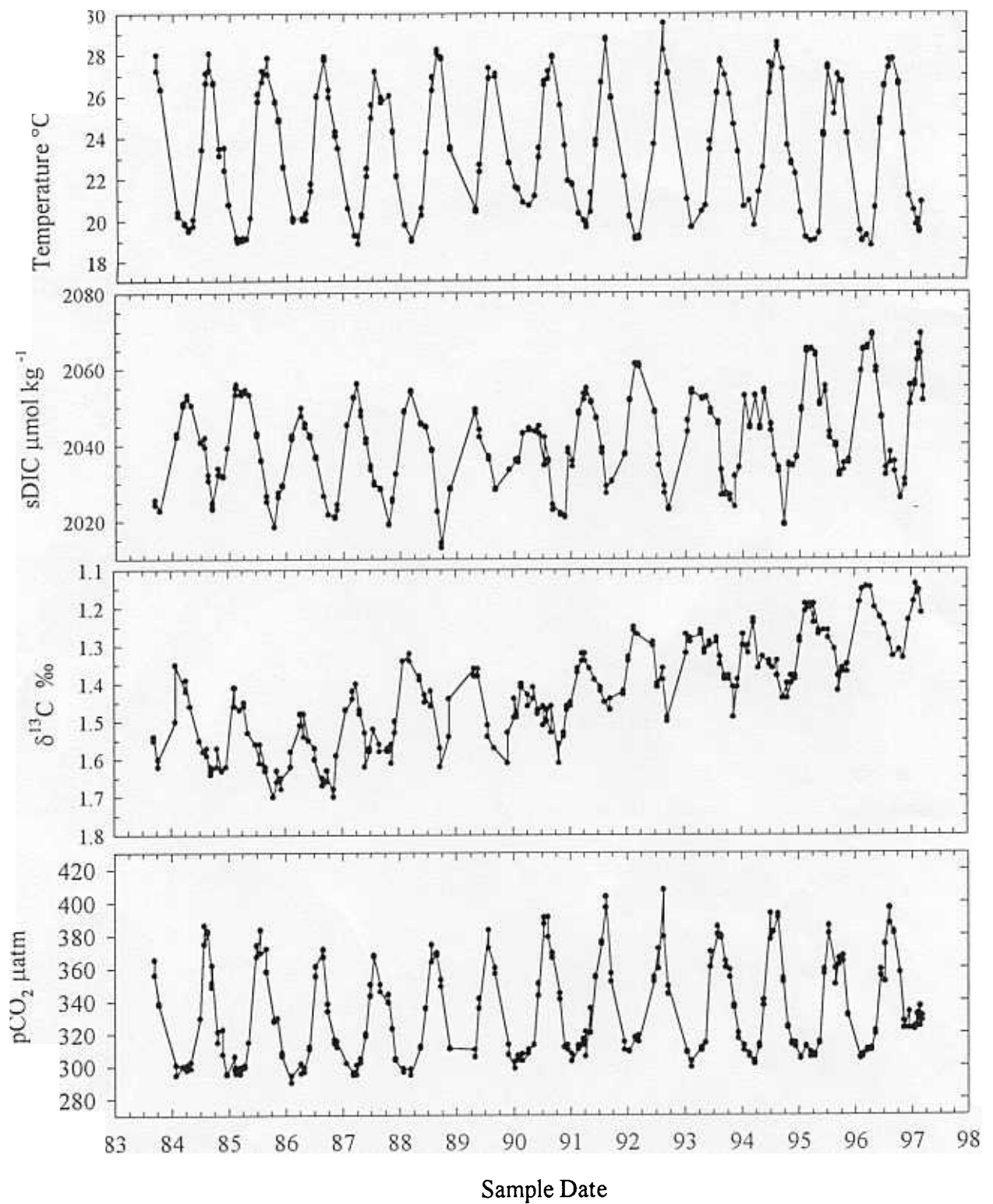
Figure B. Temperature, sDIC, $\delta^{13}C$, and pCO_2 observed at Hydrostation 'S'. The scale for the $\delta^{13}C$ data is inverted to facilitate comparison with the seasonal cycle in sDIC. The pCO_2 data were calculated from DIC, TA, temperature and salinity. Annual minima in temperature generally coincide with maxima in sDIC and minima in $\delta^{13}C$ and pCO_2.
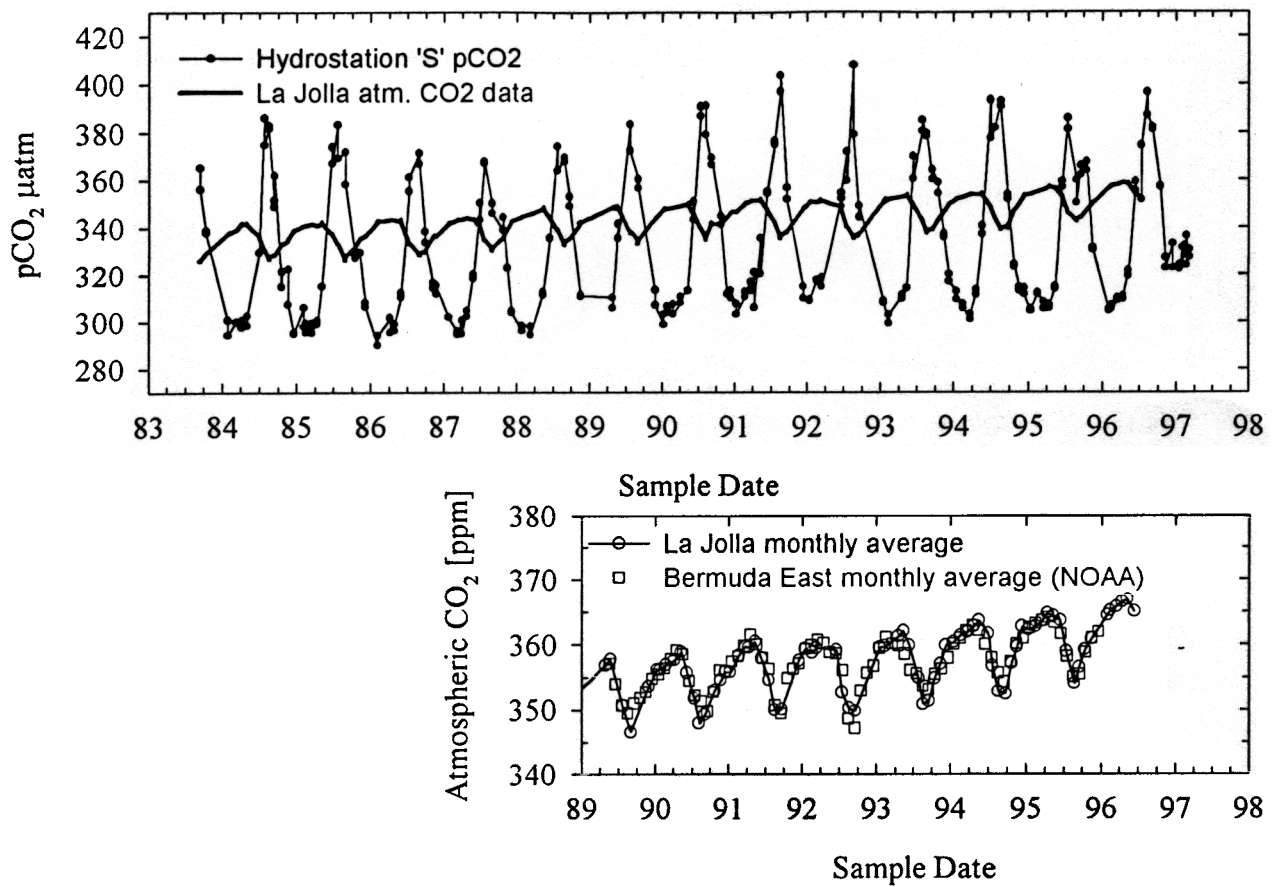
Figure C. The pCO_2 calculated from DIC and TA at Hydrostation 'S' compared to atmospheric CO_2. The atmospheric concentrations in ppm were converted to 100% relative humidity and expressed in μatm. The atmospheric CO_2 concentration data were estimated from measurements at La Jolla CA. prior to 1989. The data from La Jolla are compared to data measured at Bermuda East since 1989 in the lower figure.
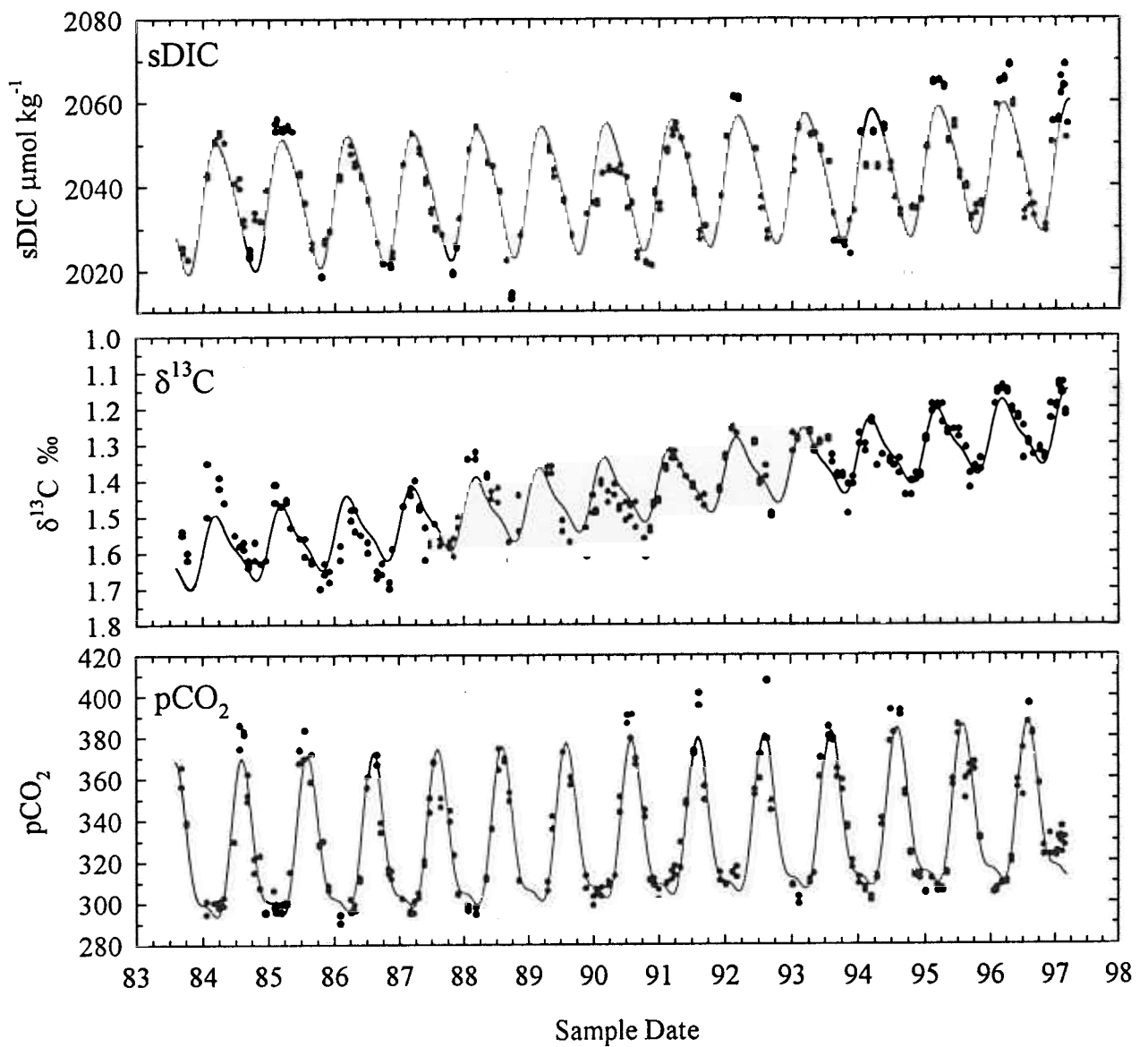
Figure D. The secular trends and seasonal cycles in sDIC, $\delta^{13}C$, and pCO_2 data were approximated by fitting the records to a linear function in time, representing the secular trend, and 6 and 12 month harmonics, representing the seasonal cycles. The resulting fits are represented by a solid line, and the data are shown as solid circles.
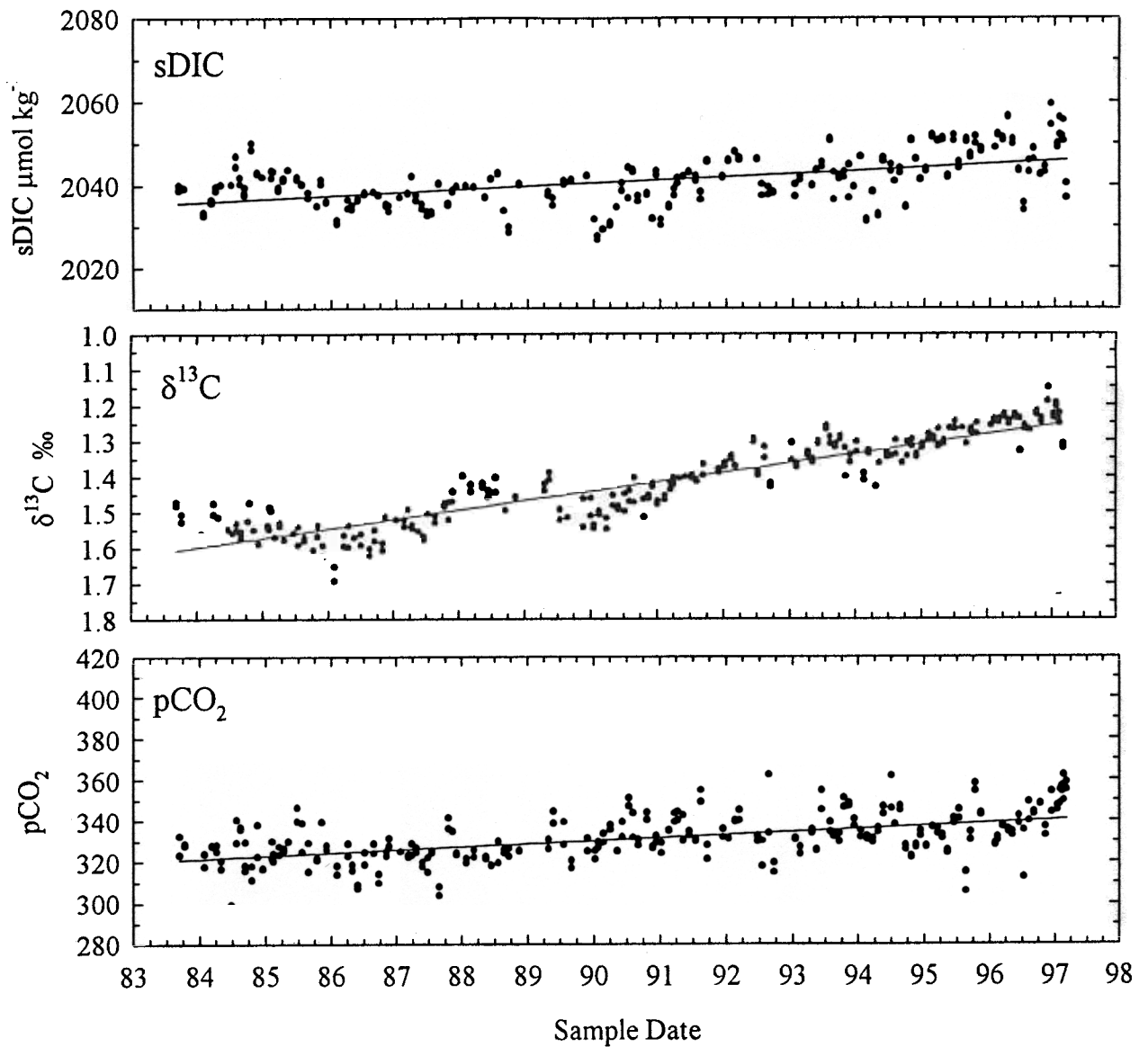
Figure E. The linear trends and fit residuals in sDIC, $\delta^{13}C$, and pCO_2 after removing the 6 and 12 month harmonics, shown in Figure D, from the records. The trends were 0.76 μmol kg^{-1} yr^{-1} -0.026 ‰ yr^{-1}, and 1.46 μatm yr^{-1} respectively.
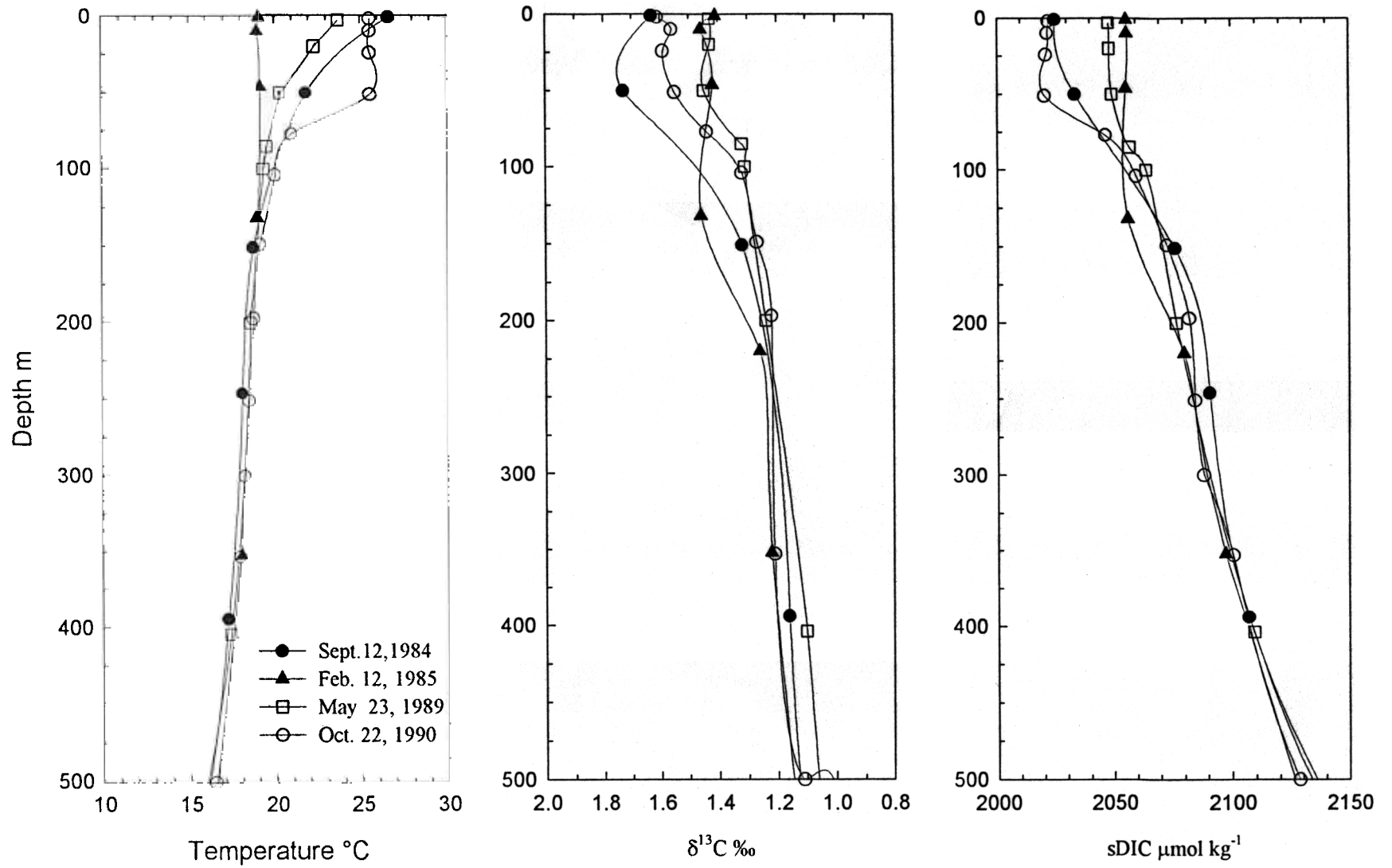
Figure F. Profiles of temperature, sDIC, and $\delta^{13}C$ sampled at Hydrostation 'S'. The development of the seasonal thermocline corresponds with decreasing sDIC and increasing $\delta^{13}C$.
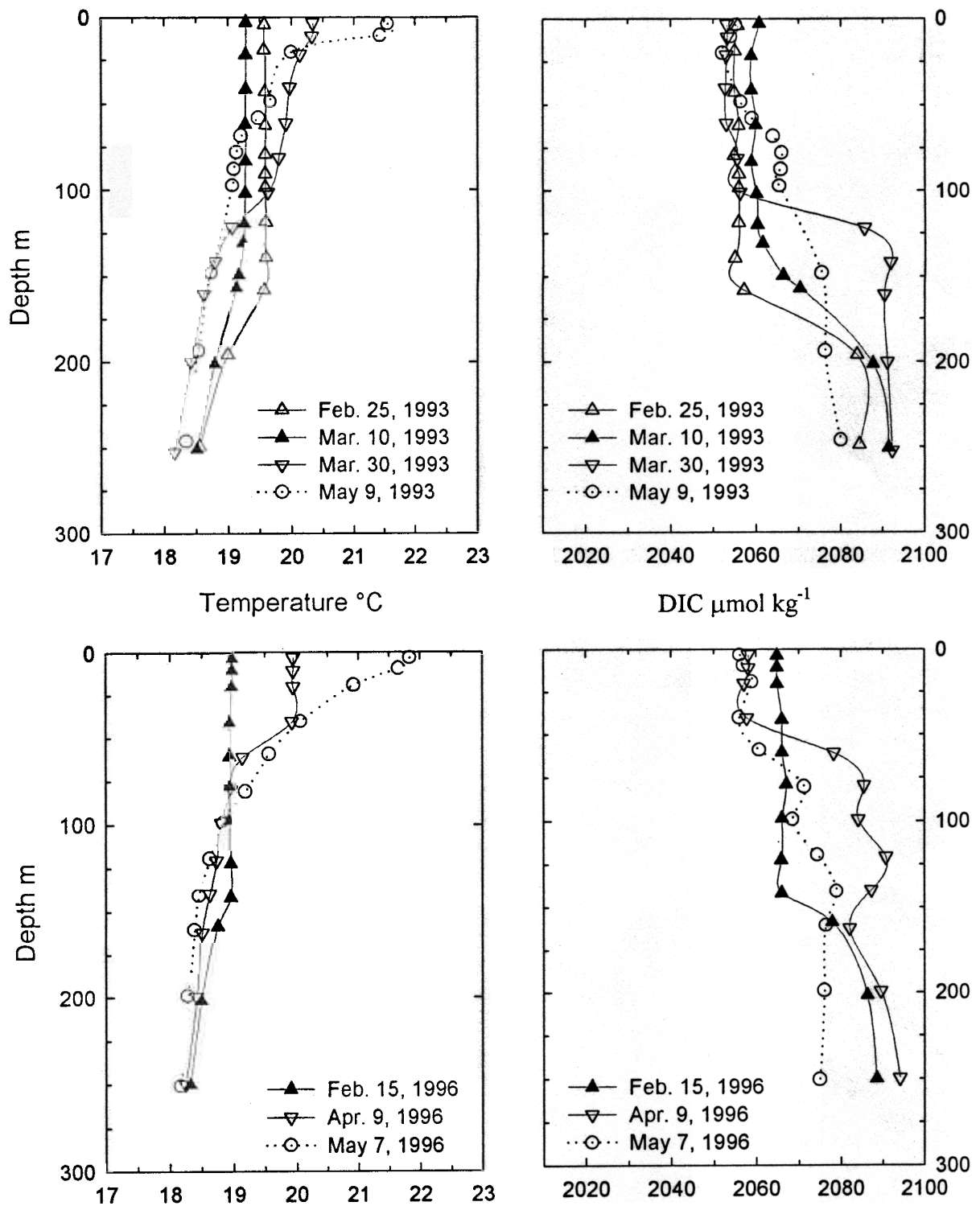
Figure G. Selected profiles in temperature and corresponding sDIC data measured at BATS.
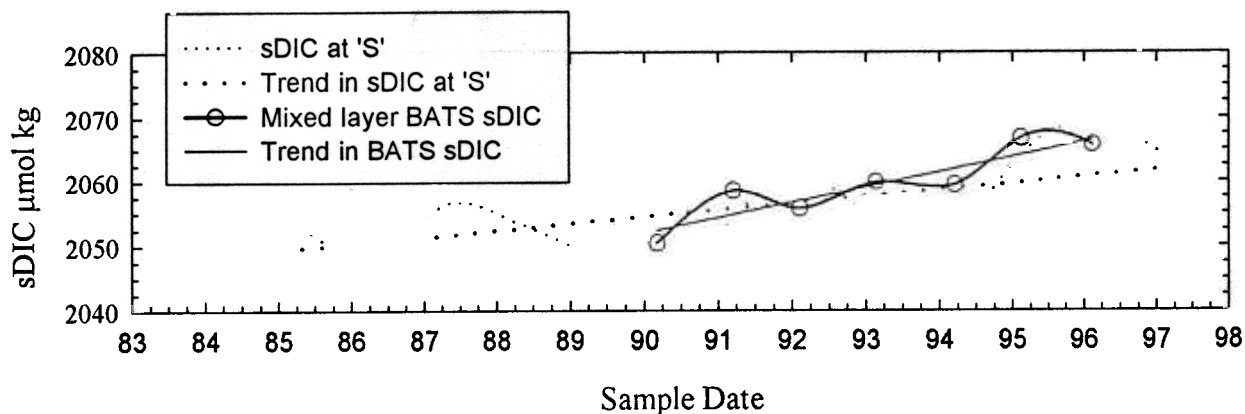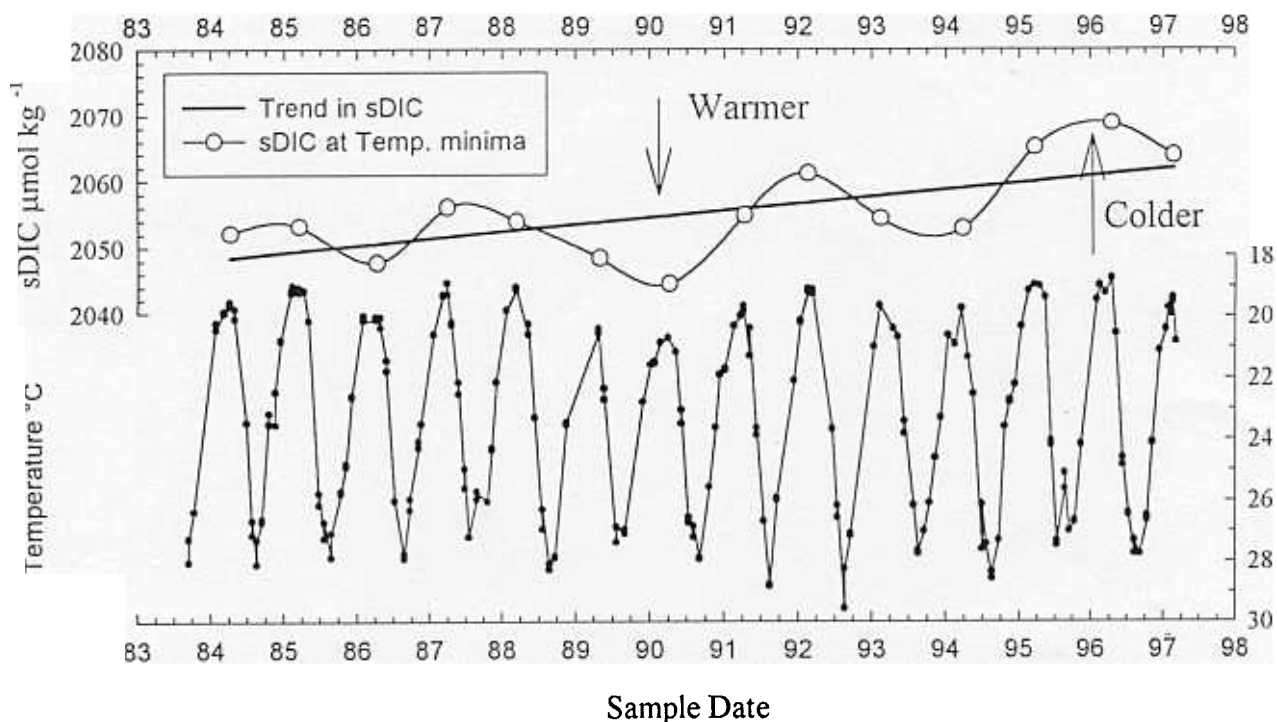
Figure H.

Upper Panel: The sDIC corresponding to annual minima in surface ocean temperature observed at Hydrostation 'S' are shown (solid symbols connected by smooth curve) with a straight line representing the secular trend. Seawater temperature is also shown, with the scale inverted to illustrate the relationship between interannual variability in sDIC and temperature.

Lower Panel: The sDIC corresponding to annual maximum in mixed layer depth at the BATS site, also generally corresponding to minima in surface ocean temperature. The sDIC were averaged over the mixed layer. The secular trend in the data, represented by a straight line, is greater than the trend observed at Hydrostation 'S' (shown by dotted lines in the figure), due to unusually low DIC values corresponding to warmer than usual temperatures at the begining of the BATS record.
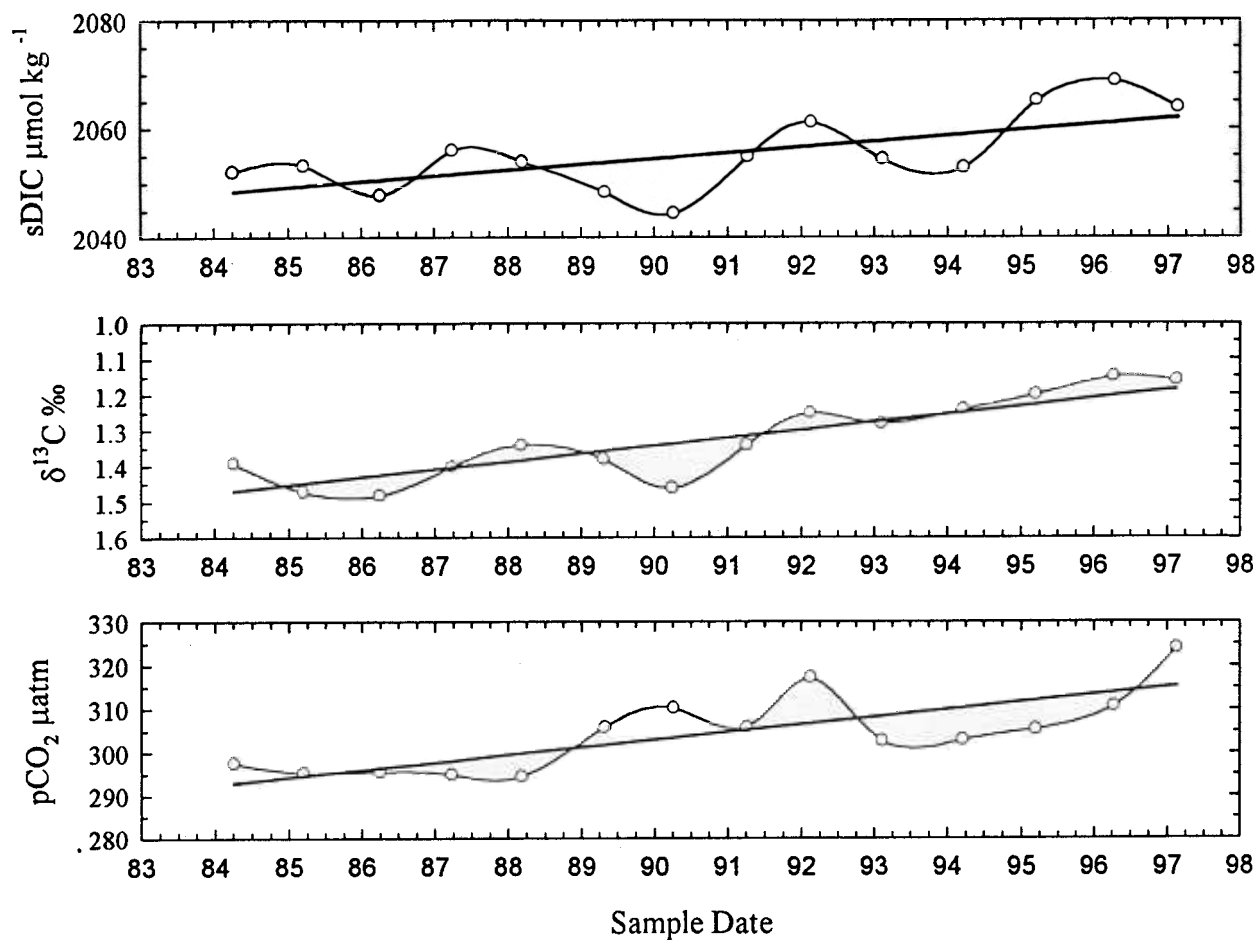
Figure I. The sDIC, $\delta^{13}C$, and pCO_2 values observed during annual minima in ocean temperature. Linear trends in the data were 0.93 μmol kg^{-1} yr^{-1}, -0.023 ‰ yr^{-1}, and 1.55 μatm yr^{-1}, respectively.

Appendix A:

Instrumentation and Procedures for DIC Analyses

Our instrumentation and techniques for measuring DIC evolved from an analysis method

developed by Wong (1970). A weighed aliquot of seawater is acidified under vacuum to convert

dissolved bicarbonate and carbonate to carbon dioxide gas. Gas extractions are performed using

vacuum extraction lines of pyrex glass, each line connected to mechanical roughing pumps in

tandem with oil diffusion pumps, as shown in Figure A1. The pumping system provides a

vacuum of about 1 millitorr. The evolved CO_2 gas is collected in a trap chilled with liquid

nitrogen. The quantity of CO_2 is determined by measuring its pressure and temperature in a

calibrated constant volume mercury manometer, as described by Keeling et al. (1986).

Extraction Procedure

Glass pipettes and extraction glassware used in our analyses are cleaned by rinsing with

deionized water supplied by a Milli-Q water purification system. After cleaning, the glassware is

baked in an oven at 550 °C for 4 hours.

Each bottle of seawater, after retrieval from storage, is warmed to room temperature

controlled to be 22 °C. Meanwhile, a glass pipette for receiving the seawater sample is evacuated,

cleaned, weighed to a precision of one milligram on a Mettler digital top-loading balance, and

attached to a filling adapter. The adapter is inserted into the sample bottle. Then, using air to

pressurize the sample at the top of the bottle, an aliquot of the water sample from near the bottom

of the bottle is forced through the pipette, filling it completely. Some water then overflows into an

overflow reservoir. After about 40 ml of sample has been dispensed through the pipette, the

lower, and then the upper, stopcocks are closed, isolating the seawater aliquot. The temperature of

the remaining sample in the bottle is recorded, and this water is retained for TA, salinity, and

inorganic nutrient analyses. The pipette ends are rinsed three times with purified (Milli-Q) water

and dried. The pipette is weighed again, and the mass of the aliquot of seawater is determined by difference.

The pipette containing the aliquot is assembled on the vacuum extraction line above a conical reaction vessel of 500 ml capacity and below a 40 ml reservoir of 1 molar, CO_2 free, aqueous solution of phosphoric acid, as shown in Figure 2. After evacuation of the reaction vessel to a pressure below 10 millitorr, Traps 1 and 2 (see Figure A1), designed in tandem for isolating the water vapor and CO_2 gas, are cooled using ethanol-dry ice slurry, and liquid nitrogen respectively. Opening the lower stopcock of the pipette causes the aliquot of seawater to flow by gravity into the reaction vessel. By closing the lower pipette stopcock and opening the upper pipette stopcock, the sample pipette fills with the phosphoric acid. The lower pipette stopcock is then opened again, draining the acid into the reaction vessel, and the solution is mixed by a magnetic stirrer. The evolved gases are slowly extracted at a pressure below 200 millitorr, as registered at Gauge G2 while vigorously stirring the solution. Gas extraction continues until the pressure measured down stream of the water vapor trap at Gauge 2 remains below one millitorr for two minutes, indicating that the CO_2 has been collected quantitatively in Trap 2. After two sublimations, employing successively Traps U1 and U2, to purify the CO_2 sample, it is frozen into a glass tube sealed with a greased stopcock. The CO_2 is stored while frozen at liquid nitrogen temperature to prevent interactions with stopcock grease prior to manometric measurement.

Manometric Measurements

The manometer system of pyrex glass consists of a permanently evacuated vertical column, a second vertical column which contains the sample during measurement, and a reservoir containing mercury. The pressure of the gas sample is measured with a precision cathetometer as the difference in heights of mercury in the two columns after correcting for height differences caused by variations in the meniscus of each column. The volume occupied by the sample during the pressure measurement is controlled, varying the height of the mercury in the sample column by pressurizing the mercury reservoir from an external source. Precisely calibrated volumes of

approximately 1, 4, 16, 64 and 250 cm^3 are defined in the sample column by glass pointers. The surface of the mercury is raised to be almost in contrast with the flattened tip of one of these pointers, and the heights of the mercury in the vacuum and sample columns are then determined using the cathetometer. This cathetometer, manufactured by Fred Henson and Co. of Pasadena in 1956, consists of a telescope mounted on a 1 mm pitch screw, which enables the mercury height to be determined to a precision of 0.005 mm.

The pressure, P, of the CO_2 gas is calculated from the difference between the two measured heights of mercury by the formula:

(1) $P = \Delta h \, \rho \, g$

where Δh denotes observed height difference in cm; ρ, the density of mercury in g cm^{-3}; and g, the acceleration of gravity at the laboratory (979.558 cm s^{-2}).

The amount of CO_2, expressed in moles, is calculated from the pressure and temperature of the CO_2 gas using a virial equation of state:

(2) $n = -[V/(2B)] \, (1 - (\, 1 + 4 \, PB/RT \,)^{1/2}$

where n represents the moles of CO_2; V denotes the calibrated volume of the manometer in cm^3; B denotes the second viral coefficient for CO_2 gas in the expansion of the compressibility factor; P is expressed in dynes cm^{-2}; and T, denotes the temperature in Kelvin (K). The gas constant, R, is set equal to 8.314510 (ergs mol^{-1}K^{-1}) (CRC, 1989, p. F-100).

The second virial coefficient is calculated using the interpolation function from values tabulated by Sengers et al. (1971);

(3) $B = 442.002 - 125548/T - 0.483343(T)$

Instrumentation and Procedure for TA Analyses

The design of the titration alkalinity (TA) instruments was based on the work of Edmond (1970), the GEOSECS titration systems (Bradshaw et al., 1981) and the recommendations of Dickson (1981), and is shown in Figure 3. The seawater samples remaining after analysis of aliquots for DIC, as described above, are titrated in a closed, jacketed, glass cell. A Dosimat burette system (Metrohm model 655), with a precision glass tip, delivers titrant to the cell. The cell voltage (e.m.f.) is measured by an Orion combination electrode (model 81-02) immersed in the solution, a high impedence voltage follower, and a Hewlett Packard (HP) voltmeter (model 3478A) with one microvolt sensitivity. The cell compensates for the additional titrant volume by compressing a flexible vinyl bladder inserted into the solution. The titrations are controlled using a Hewlett-Packard HP 86B desktop computer connected to the Dosimat and to the voltmeter. For each titration step, the computer dispenses the titrant, and recorded the titrant volume, e.m.f. data, and time at one second intervals. The titrant is prepared in batches of between 4 and 20 liters using a concentrated HCl solution (Fisher cat # SA49) and Milli-Q water, at a concentration of nominally 0.22 mol kg-1. Reagent grade sodium chloride (Fisher #S271-10) is added to the titrant to give a precisely determined total ionic strength of approximately 0.7 (Dyrssen and Sillen, 1967).

Titration Procedure

A clean sample bottle is fitted with a fill adapter, shown in Figure 3, and weighed on a Mettler digital top-loading balance to a precision of 0.01 g. The titration cell, rinsed several times with Milli-Q water after the previous titration, is assembled with a mercury thermometer and the burette tip. The sample is dispensed into the cell by pressurizing the head-space with nitrogen gas while observing the solution-level through an opening in the cell top. When the cell is nearly full, the pressure in the bottle is reduced to ambient, and the cell top is stoppered, trapping about 5 ml of air in contact with the solution. The sample bottle is weighed again, and the weight of solution dispensed into the cell is determined by difference, typically 170 to 180 grams. After recording

the temperatures of the cell and of the titrant, the e.m.f. is monitored for 1 to 5 minutes until the cell temperature is within 0.5 °C of the cooling bath temperature. The titration begins by adding the titrant in 0.100 ml increments. During the titration the e.m.f. and temperature are recorded once per second, beginning two seconds after the titrant addition. The extent of reaction, observed as the rate of change in e.m.f., is monitored for each titration step. A change in e.m.f. not greater than 10 microvolts over a 5 second interval is considered to indicate that the solution has attained equilibrium with the titrant, and after 3 such increments were recorded, the next titrant increment is delivered. More closely spaced measurements are taken near the alkalinity equivalence point (between 1.6 to 2.0 ml total volume of titrant) by reducing the titrant increments to 0.020 ml. The final total volume of titrant added varies from 2.2 to 3.0 ml. A complete titration takes about 30 minutes.

The titration data are processed using a non-linear least squares minimization procedure (Dickson, 1981; DOE, 1994). Further details regarding the fitting of TA data, including the equations used in the fitting program, are provided in Appendix A.

Instrumentation and Procedure for $^{13}C/^{12}C$ analyses

After each manometric measurement for DIC, the CO_2 of the sample is sublimed into a previously annealed and flame-sterilized pyrex glass tube. The CO_2 transfer takes place under vacuum, the sample being frozen into the bottom of the tube using liquid nitrogen. The glass tube is sealed 6 to 7 cm above the frozen CO_2, using a gas and oxygen torch, and then stored until mass spectrometric analysis when the tube is cracked open in an apparatus mounted on the mass spectrometer and the gas transferred to the spectrometer inlet system.

Standardization Techniques

The reliability of time series measurements depends on repeated standardization of all laboratory procedures. The vacuum extraction procedure for DIC was checked by manometric

assay of ultrapure anhydrous solid sodium carbonate (Baker Ultrex catalog # 4923-04). The standardization of the mercury manometer is described by Keeling et al. (1986).

As a primary standardization of TA, analyses of seawater are compared with titrations of standard solutions containing sodium carbonate and sodium chloride in Milli-Q water, as described above. The solutions are prepared by drying both salts at 280 $^{\circ}$C to constant weight, then weighing aliquots of these salts and of Milli-Q water into one liter bottles made of vitreous quartz and equipped with greased stoppers. Batches of sodium chloride have been found to contain variable trace amounts of alkalinity which are determined by coulometric titration. The standard solutions are titrated identically to seawater samples.

Bicarbonate standard solutions, used as daily working standards for TA determinations, are prepared in 20 to 50 liter batches using sodium carbonate, sodium chloride, and Milli-Q water, as with the carbonate standards. Filtered and humidified laboratory air is pumped through the solution for 5 to 7 days until the pH stabilizes at about 8.2. The solutions are bottled in vitreous quartz or pyrex type glass bottles, poisoned with 0.1 ml of saturated $HgCl_2$ solution, and sealed with greased stoppers. Standard solutions were prepared with sufficient regularity to overlap analyses of successive batches, thus insuring the integrity of the time series TA analyses.

Our principal isotopic standards for calibration of the VG prism isotope ratio mass spectrometer at the Scripps Institution of Oceanography are two standards of pure CO_2 gas stored in 0.5 L stainless steel cylinders, GS19 and GS20, supplied to us by the Groningen Laboratory. Three additional gas standards are obtained by extracting CO_2 from air stored under high pressure in steel cylinders with a capacity 6000 liters, at standard pressure and temperature. All five standards, also used to calibrate ^{13}C / ^{12}C measurements of atmospheric CO_2, have been compared by direct mass spectrometic analysis to primary standards of CO_2 derived from the international isotopic standards NBS-16, NBS-17, and NBS-19. The NBS standards have been assigned values for $\delta^{13}C$ using the data of Coplen et al. (1983). The results are corrected according to the relations of Craig (1957) as described by Bollenbacher et al. (1998).

The standards extracted from air contain N_2O which influences the determination of $\delta^{13}C$ (Mook and van der Hoek, 1985). For calibration of seawater samples we have employed these standards only to make day to day corrections to the mass spectrometer calibration. Slow drifts in these air standards, compared to the pure CO_2 standards, were corrected for to make all five standards compatible for daily calibration purposes, assuming that the pure CO_2 standards were perfectly stable.

Calibrations of samples run in the Groningen laboratory were carried out by procedures described by Mook et al. (1983), based on a suite of international and laboratory standards. The calibration data for samples from 1984 through 1990 have not been published. Calibrations carried out at the Scripps Institution of Oceanography are described by Bollenbacher et al. (1998).

Appendix Table 1. Equations used to calculate seawater equilibrium expressions referred to in the text. The primary source of the equation is listed first, followed by the reference (if different) which details the experimental method used to obtain the equation.

Source	Equation
	Equations which relate concentrations to seawater salinity
Uppstrom,1974	$B_T = (0.000232/10.811)(S/1.80655)$
Morris and Riley, 1966	$S_T = ((0.1400/96.062)*S/1.80655)$
Riley, 1965	$F_T = (0.000067/18.998)*S/1.80655$
	non-CO_2 equilibrium constant expressions
DOE, 1994; Millero, 1995	$\ln K_W = -13847.26/T + 148.96502 - 23.6521\ln(T) + (118.67/T - 5.977 + 1.0495\ln(T))S^{1/2} - 0.01615S$
DOE, 1994; Dickson, 1990b	$\ln K_B = (-8966.9 - 2890.53S^{1/2} - 77.942S + 1.728S^{3/2} - 0.0996S^2)/T + (148.0248 + 137.1942S^{1/2} + 1.62142S) + (-24.4344 - 25.085S^{1/2} - 0.2474S)\ln(T) + 0.053105S^{1/2}T$
DOE, 1994; Dickson, 1990a	$\ln K_S = -4276.1/T + 141.328 - 23.093\ln(T) + (-13856/T + 324.57 - 47.986\ln(T))(i)^{1/2} + (35474/T - 771.54 + 114.723\ln(T))(i) - 2698i^{3/2}/T + 1776(i^2)/T + \ln(1 - 0.001005S)$; where $(i) = 19.924S/(1000 - 1.005S)$
DOE, 1994; Dickson and Riley, 1979	$\ln K_F = (1590.2/T - 12.641 + 1.525(i^{1/2}) + \ln(1 - 0.001005S) + \ln(1+S_T/K_S))$; where $(i) = 19.924S/(1000 - 1.005S)$
	Solubility of CO_2
DOE, 1994; Weiss, 1974	$\ln K_0 = -60.2409 + 93.4517(100/T) + 23.3585(\ln(T/100)) + S(0.023517 - 0.023656(T/100) + 0.0047036(T/100)^2)$
	CO_2 equilibrium constants
Lueker et al., 2000 (Marine Chem)	$pK_1 = 3633.86 / T - 61.2172 - 0.011555\ S + 0.0001152\ S^2 + 9.6777\ \ln(T)$
Lueker et al., 2000 (Marine Chem)	$pK_2 = 471.783 / T + 25.9289 - 0.017811\ S + 0.0001123\ S^2 - 3.1697\ \ln(T)$